Front. Optoelectron. 2020, 13(1): 50–72
https://doi.org/10.1007/s12200-019-0949-7

REVIEW ARTICLE

Topological photonic crystals: a review

Hongfei WANG[1], Samit Kumar GUPTA[1], Biye XIE[1], Minghui LU (✉)[1,2,3]

1 National Laboratory of Solid State Microstructures and Department of Materials Science and Engineering, Nanjing University, Nanjing 210093, China
2 Collaborative Innovation Center of Advanced Microstructures, Nanjing University, Nanjing 210093, China
3 Jiangsu Key Laboratory of Artificial Functional Materials, Nanjing University, Nanjing 210093, China

Abstract The field of topological photonic crystals has attracted growing interest since the inception of optical analog of quantum Hall effect proposed in 2008. Photonic band structures embraced topological phases of matter, have spawned a novel platform for studying topological phase transitions and designing topological optical devices. Here, we present a brief review of topological photonic crystals based on different material platforms, including all-dielectric systems, metallic materials, optical resonators, coupled waveguide systems, and other platforms. Furthermore, this review summarizes recent progress on topological photonic crystals, such as higher-order topological photonic crystals, non-Hermitian photonic crystals, and nonlinear photonic crystals. These studies indicate that topological photonic crystals as versatile platforms have enormous potential applications in maneuvering the flow of light.

Keywords topological photonic crystals, topological phase transitions, non-Hermitian photonics, higher-order topological photonic crystals

1 Introduction

A deep understanding of the physical properties of materials is fundamental in many of the essential breakthroughs in science and technology. Over the past few decades, topological photonic crystals have opened a new frontier to optical propagation and manipulation. Various physical mechanisms and optical phenomena have been explored due to topological properties of band structures in photonic crystals, which greatly promote the development of this field.

Photonic crystals are periodic optical structures that modulate the motion of photons, in which the periodic dielectric material is the analogous of atoms or molecules in conventional crystals. It was first proposed in 1987 by Yablonovitch [1] and John [2], afterwards, its properties such as forbidden bang gap [3,4] and negative refraction [5,6] have been studied extensively. In another aspect, the concepts of topological phases of matter can be traced back to the integer quantum Hall effect (IQHE) discovered in 1980. In the IQHE [7], a two-dimensional (2D) electron gas exhibits quantized Hall conductance, which is a function of the magnitude of magnetic fields and equals to the integer multiple of e^2/h. In 1982, Thouless et al. [8,9] proposed that the quantized Hall conductance is characterized by a nonzero topological invariant (the Chern number or Thouless, Kohmoto, Nightingale, and Nijs (TKNN) number) of this system. After that, Kane and Mele [10–13] discovered a new class of topological phases of matter known as the quantum spin Hall effect (QSHE) in 2005. In this system, the Chern number is zero while the wave function is classified by a nonzero binary topological invariant under time-reversal symmetry (TRS). Since then, many different kinds of topological phases of matter have been extensively investigated under various symmetries.

Parallel to the development of condensed matter physics, Haldane and Raghu [14,15] realized that topological phases are in fact a ubiquitous phenomenon of waves in the periodic medium, and they predicted that topologically protected boundary states will exist in the 2D periodic structure of magneto-optical elements. In the next year (2009), the idea was experimentally proved by using the 2D magneto-optical photonic crystal [16]. A clear nontrivial band structure was indeed found in this system, corresponding to a unidirectional topological edge state. However, the limited magneto-optical response calls for large magnetic fields, which is not conducive to the system integration. In 2011, Hafezi et al. considered the pseudospin degree of freedom of photons and found the quantum spin Hall effect of the optical system [17–24],

Received June 25, 2019; accepted October 16, 2019

E-mail: luminghui@nju.edu.cn

where the TRS is maintained and artificial magnetic fields act on each pseudospin. Later, Fang et al. [25–34] provided another idea (Floquet topological insulators), where the dynamic modulation generates an effective time-independent Hamiltonian with broken TRS in 2012. Since then, a lot of research endeavors have been put in unravelling novel band structures and optical phenomena in topological photonic crystals, such as valley photonic crystals [23,35,36] and 3D topological insulators [37,38]. In addition, the topological properties of band structures also involve the band degeneracies which can be regarded as gapless materials (i.e., semimetals) in photonics such as Dirac semimetals [39–41], Weyl semimetals [42,43] and nodal line semimetals [44,45], which show the great potential to reveal physical properties and control the transport of surface states [42,43,46] (e.g., Fermi arc and negative refraction).

Most recently, there has been a great activity in various aspects of topological photonic crystals such as nonlinear systems [26,47–60], non-Hermitian systems [61–82], and higher-order topological systems [83–98]. This is because the study of topological phases of traditional photonic crystal systems is closely related to the development of condensed matter physics. Researchers have begun to study the topological photonic crystals from the point of view of rich physical properties of photons. Utilizing unique photonic effects, the study of topological photonic crystals will greatly improve the optical applications and enrich the content of topological physics.

In this review, we classify topological photonic crystals by material platforms and summarize some novel concepts such as higher-order topological photonic crystals, machine learnings, and topological Fano resonances for the first time. We focus on the developments of topological photonic crystals, the material platforms, and the corresponding topological properties. The content is divided into five sections including an introduction in Section 1. The basic concepts of photonic systems and topological phase transitions are discussed in Section 2. Section 3 introduces the photonic crystals of various material platforms and their topological phases while novel achievements of topological photonic crystals in recent times are highlighted in Section 4. In the last section, we summarize the review and discuss the outlook for this field.

2 Basic concepts

In this section, the general concepts of photonic systems and topological phases of matter are formulated. This section is divided into two parts. We briefly review the features of photonic systems for topological photonic crystals in the first part. Then in the second part, the topological phase transitions of matter are discussed in more details.

2.1 Photonic systems

The development of topological phases raises from the electric conducting experiment in condensed matter. A significant difference between electronic systems and photonic systems is that the former is fermionic, while the latter is bosonic. The major prominent difference between them is illustrated in Fig. 1. As can be seen, they possess different TRS operators: $T_f = \mathrm{i}\sigma_y K$ for electrons $T_f^2 = -1$ and $T_b = \sigma_z K$ for photons $T_b^2 = 1$, where σ_y and σ_z are the Pauli matrixes, K is the complex conjugation operator. In addition, due to the Pauli exclusion principle, the noninteracting fermions fill all the states below the Fermi level with only one particle per state at low temperatures, and all higher energy states remain empty. However, the presence of losses and the modulation of propagation make it different in photonic systems, so that the ground states of whole systems are trivial vacuum states that maintaining and generating the photon in a state of interesting topological features requires injecting light from the external source.

On the other hand, nonlinear effects give rise to many important physical attributes in photonic systems. The standard nonlinear optical processes are semiclassically described by Maxwell's equations, which include the nonlinear terms raising from nonlinear dielectric polarization. The dielectric polarization can be written in the form [99–101]

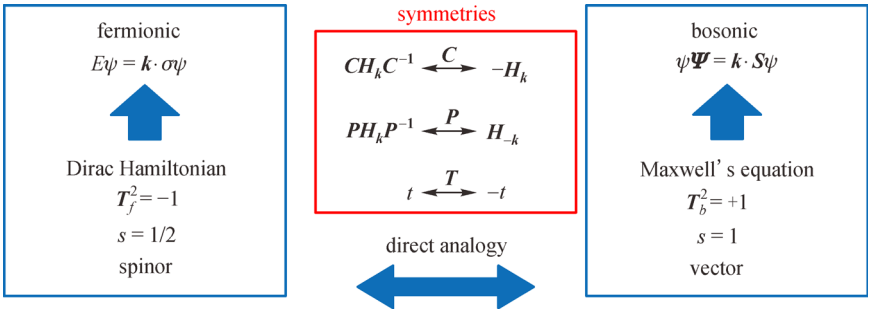

Fig. 1 Direct analogy between electrons (fermionic) and photons (bosonic) systems

$$P = \varepsilon_0(\chi^{(1)} \cdot \boldsymbol{E} + \chi^{(2)} : \boldsymbol{EE} + \chi^{(3)} \vdots \boldsymbol{EEE} + ...). \quad (1)$$

Here, ε_0 is the dielectric constant of vacuum, and $\chi^{(1)}$, $\chi^{(2)}, \chi^{(3)}$ correspond to linear, second-order and third-order susceptibility, respectively. The linear susceptibility is expressed as the usual refractive index. The second-order susceptibility is expressed as second harmonic generation [102–105], parametric down-conversion processes [106–110], etc. The third-order susceptibility leads to third harmonic generation [111–115], four-wave mixing processes [116–119] and nonlinear refractive index [47,120,121]. As the simplest properties of $\chi^{(3)}$, the nonlinear refractive index is defined by

$$\tilde{n} = n_0 + \tilde{n}_2|\boldsymbol{E}|^2. \quad (2)$$

Here, n_0 is the linear refractive index and $\tilde{n}_2$ is related to $\chi^{(3)}$, the nonlinear refractive index depends on the intensity of light. Most of the topological phase transitions witnessed are inspired by $\chi^{(2)}$ or $\chi^{(3)}$ terms in nonlinear photonic crystals. In the quantitative point of view, the nonlinear effects of common materials lead to very weak interactions for single photons, therefore it can be described by the mean-field approach. For $\chi^{(3)}$ terms, this means $\langle \hat{E}^\dagger(\boldsymbol{r}), \hat{E}(\boldsymbol{r}), \hat{E}(\boldsymbol{r})\rangle \cong \langle \hat{E}^\dagger(\boldsymbol{r})\rangle \langle \hat{E}(\boldsymbol{r})\rangle \langle \hat{E}(\boldsymbol{r})\rangle$, here $E(\boldsymbol{r}) = \langle \hat{E}(\boldsymbol{r})\rangle$. In this approach, the imaginary part of $\chi^{(3)}$ and $\tilde{n}_2$ can also be included in their motion. For strong nonlinearities, main research aims to set up such strongly interacting systems. An effective mechanism is that polaritons in coherently driven atomic gases can be controlled by the electromagnetically induced transparency (EIT) in Rydberg states (Rydberg polaritons or circle-QED) [56,122].

2.2 Topological phase transitions of matter

The first influential experimental observation of topological phase transitions is the QHE in electron gas systems. Shortly afterwards, the quantization of the Hall conductance was identified with the topological phase of bands in momentum space by Thouless, Kohmoto, Nightingale, and Nijs (TKNN) [8,9]. The topological properties of a band depend in part on the eigenvalues $E_n(\boldsymbol{k})$, but also on the eigenvectors $\varphi_{n,k}(\boldsymbol{r})$ as a function of $\boldsymbol{k}$. This geometric phase of eigenvectors is called Pancharatnam-Berry phase [123,124]. The specific expression is defined in the following.

$$\gamma_n = \oint \mathcal{A}_n(\boldsymbol{k}) \cdot \mathrm{d}\boldsymbol{k}, \quad (3)$$

where the Berry connection is defined as $\mathcal{A}_n(\boldsymbol{k}) = \langle \varphi_{n,k}|\nabla_k|\varphi_{n,k}\rangle$ and the integral for a given closed path leads to a gauge-invariant variable. $\mathcal{A}_n(\boldsymbol{k})$ can also form a gauge Berry curvature $\Omega_n(\boldsymbol{k}) = \nabla_k \times \mathcal{A}_n(\boldsymbol{k})$. It is worth noting that the Berry curvature is continuously defined over the whole Brillouin zone and the phase of eigenvectors cannot always to be continuous. So a topological invariant (Chern number) is defined as the integral.

$$C_n = \frac{1}{2\pi}\int_{\mathrm{BZ}} \mathrm{d}^2\boldsymbol{k}\Omega_n(\boldsymbol{k}). \quad (4)$$

According to Stokes' theorem, the nonzero Chern number implies that the eigenvector and Berry connection cannot be continuously defined. With the noninteracting linear response, the Hall conductance of the two-dimensional insulator is

$$\sigma_{xy} = -\frac{e^2}{h}\sum\nolimits_n C_n. \quad (5)$$

Here, the Chern numbers are summed over the n occupied bands, which leads to quantized conductance in units of e^2/h. However, the TRS is broken in these models so far, which means the Berry curvature violates $\Omega_n(-\boldsymbol{k}) = -\Omega_n(\boldsymbol{k})$ for nondegenerate bands. For degenerate bands, a similar argument also establishes that there is no Chern bands can be found in 2D systems with TRS. After this, the quantum spin Hall system was proposed by Kane and Mele in 2005 [10]. This system consists of two copies of the Chern topological insulators, and the magnetic fields acting on two opposite spins, where spin up C_{up} is opposite to spin down C_{down}. Since the magnetic fields are opposite for two spins, the TRS is preserved and the sum of Chern numbers is zero. Thus it is also called the $\mathbb{Z}_2$ topological insulator, which takes topological invariants ($C_{\mathrm{up/down}}$ mod 2) of either 0 (trivial) or 1 (nontrivial). Analogous to quantum spin Hall insulators in the electron gas, the polarization degree of freedom can be constructed as pseudospins in photonic systems. In general, the topological properties of band structures not only depend on global topological invariants (e.g., global Chern number) over the Brillouin zone [16,125], but also are influenced by local topological invariants (e.g., valley Chern number whose sign is opposite for K and K' points of the Brillouin zone, but the Chern number for the whole band is still zero) [23,36]. Both of them possess backscattering-immune edge states to some extent but protected by different topological features [16,35].

Topological gapless systems with degenerate points (i.e., Dirac or Weyl points) or lines (i.e., nodal lines) are protected by specific symmetries, and are topologically stable in momentum space. For Dirac semimetals, the most prominent feature is the non-trivial Berry phase $\pm\pi$, which means their eigenvectors are transported adiabatically on a closed loop around Dirac points [39–41]. By integrating the Berry curvature in a 2D surface enclosing a Weyl point, the topological properties of each Weyl points can be associated with a nonzero topological invariant (± 1) in Weyl semimetals. The emergence of this system requires breaking at least one symmetry between P and T, and

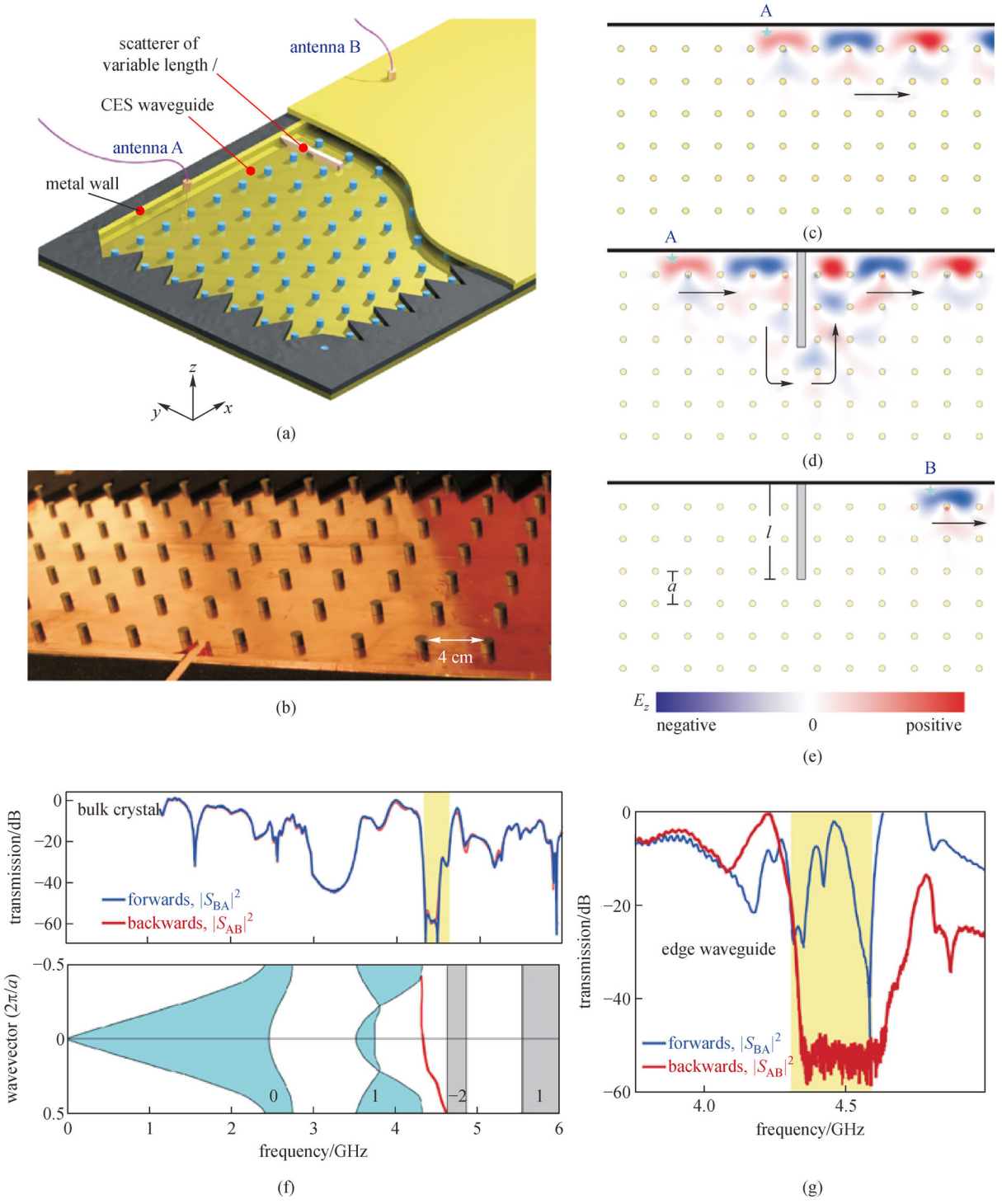

Fig. 2 (a) Gyromagnetic photonic crystal used in experiments. The blue rods indicate the gyromagnetic material and 0.2T magnetic field is applied along the z direction; (b) top view of actual waveguides; (c), (e) unidirectional and non-reciprocal propagation; (d) robust propagation against backscattering; (f) reciprocal transmission measured using the bulk photonic crystal and the projected dispersion including bulk and edge states; (g) non-reciprocal transmission via chiral edge states. Reproduced from Ref. [16]

is reflected in the topologically surface states in 3D systems [42,43,126–128]. In 3D nodal line semimetals, nodal lines are proven to be protected by PT symmetry with Berry phase π ($\mathbb{Z}_2$ charge), similar to 2D Dirac cones [129]. Surface states of this system are protected by T and screw rotation symmetry and carry non-trivial Chern numbers.

3 Various photonic crystal platforms

After having a basic understanding of photonic systems and topological phase transitions of matter, the present section is focused on the topological photonic crystals with different material platforms. Starting from the all-dielectric photonic crystal, this section also moves to photonic crystals containing metal structures, optical resonator lattices and photonic crystals of coupled waveguide systems and finally, other proposals.

3.1 All-dielectric photonic crystals

Since there are no additional losses and advantages for structural integration, all-dielectric photonic crystals provide a unified platform for studying topological phase. The QHE of electromagnetic wave system was first confirmed experimentally by Wang et al. in 2009 [16]. The sample is made up of 2D magneto-optical photonic crystals and is measured in the microwave domain as shown in Fig. 2. The unidirectionally propagating edge states can be found in the bandgap, and the gap Chern number $C_{\text{gap}} = 1$. In 2015, Skirlo et al. performed microwave measurements in the edge and bulk of ferromagnetic photonic crystals, and large Chern numbers $C_{\text{gap}} = 2$, 3, 4 are present in the experiment [125], which further the understanding of the QHE effect in photonic systems.

Quantum spin Hall effects for all-dielectric photonic crystals can also be realized in two classical ways. One way is to design a photonic crystal structure with crystalline symmetries. Wu and Hu [21] first proposed this method in the honeycomb lattice in 2015. Figures 3(a), 3(b) and 3(c) show the structural design and numerical simulation. The dielectric rods are arranged in the honeycomb lattice and formed the two-sites unit cell, which results in the Dirac dispersion at K and K' points. If we consider the hexagonal area as the unit cell, the band folding translates the Dirac points to the Γ point which leads to a doubly degenerate Dirac cone. The p_x and p_y characters are presented for the lower doubly degenerate bands, while the upper two bands presented d_{xy} and $d_{x^2-y^2}$ symmetries. Using symmetric and antisymmetric modes combination, the pseudospin basis can be constructed as $p_\pm$, $d_\pm$ and the bands possess nonzero pseudospin Chern numbers. Generally, Maxwell's equation represents the bosonic systems ($T_b^2 = 1$), however an antiunitary operator can be constructed in this system, $T^2 = (KT)^2 = -1$ where K represent the parity of p (π/2 rotation) and d (π/4 rotation).

Another way is to construct a photonic crystal using bianisotropic metamaterials [19,37,132,133]. The unique advantage of this material is the enhanced flexibility for the effective dielectric permittivity ε, magnetic permeability μ, and magnetoelectric coupling χ. This idea was first proposed by Khanikaev et al. in 2013, and the electric and magnetic response can be written in the form [19]

$$\begin{pmatrix} D \\ B \end{pmatrix} = \begin{pmatrix} \varepsilon & \mathrm{i}\chi_1 \\ -\mathrm{i}\chi_2 & \mu \end{pmatrix} \begin{pmatrix} E \\ H \end{pmatrix}. \tag{6}$$

The key theoretical insight stems from the condition $\varepsilon = \mu$, so that the TE and TM polarized modes have the same wavenumbers $\boldsymbol{k}$ and $(E,H) \rightarrow (-H,E)$. For a given $\boldsymbol{k}$, the $\varphi_{\boldsymbol{k}}^{+}$ can be transformed into $\varphi_{-\boldsymbol{k}}^{-}$ by a symmetry operation D, a similar way as the TRS of electron's spin, here $D^2 = -1$. Then, the magneto-electric coupling χ generates a strong spin-orbit coupling of pseudospins. When $\chi_1 = \chi_2 \neq 0$, the doubly degenerate Dirac points are gapped out and this topological property is protected by D. Such quantum spin Hall effects of photonic systems have been observed in microwave frequencies by Chen et al. in 2014 [132]. After this, three-dimensional (3D) bianisotropic photonic crystals also have been proposed by Slobozhanyuk et al. in 2017 [37], as shown in Figs. 3(d), 3(e) and 3(f).

Topological photonic crystals that exhibit quantum valley Hall effects may offer great application aspects in optical communications [35,134] and integrated optical devices [134], even though corresponding edge states may not robust against all kinds of spatial disorders. Quantum valley Hall effects arise from two Dirac points at K and K' points in a graphene-like lattice. The Dirac Hamiltonian at two inequivalent points express as $H_{\text{D}} = \pm\nu_{\text{D}}(\sigma_x \delta k_x + \sigma_y \delta k_y) \pm \gamma\sigma z$, here $\delta\boldsymbol{k} = \boldsymbol{k} - K$ is the reciprocal vector, ν_{D} and $\sigma_{x,y,z}$ denote the group velocity and three Pauli matrices, and γ denotes the inversion asymmetric between two sublattices. For $\gamma \neq 0$, nonzero valley Chern numbers with opposite signs appear at K and K' respectively (although the global Chern number for the band always being zeros). Valley edge states exist at the interface between two different structures with opposite signs γ and $-\gamma$. In 2017, Chen et al. proposed the idea of all-dielectric photonic crystals realizing valley Hall effects [135], the corresponding experiment was confirmed later [136]. In 2019, Shalaev et al. achieved the valley topological transport based on silicon photonic crystals at telecommunication wavelengths [134]. Since band structures and projected dispersions can be controlled below the air dispersion, the valley Hall effects achieved in slabs may find applications in optical telecommunications devices.

In parallel to the above investigations, topological

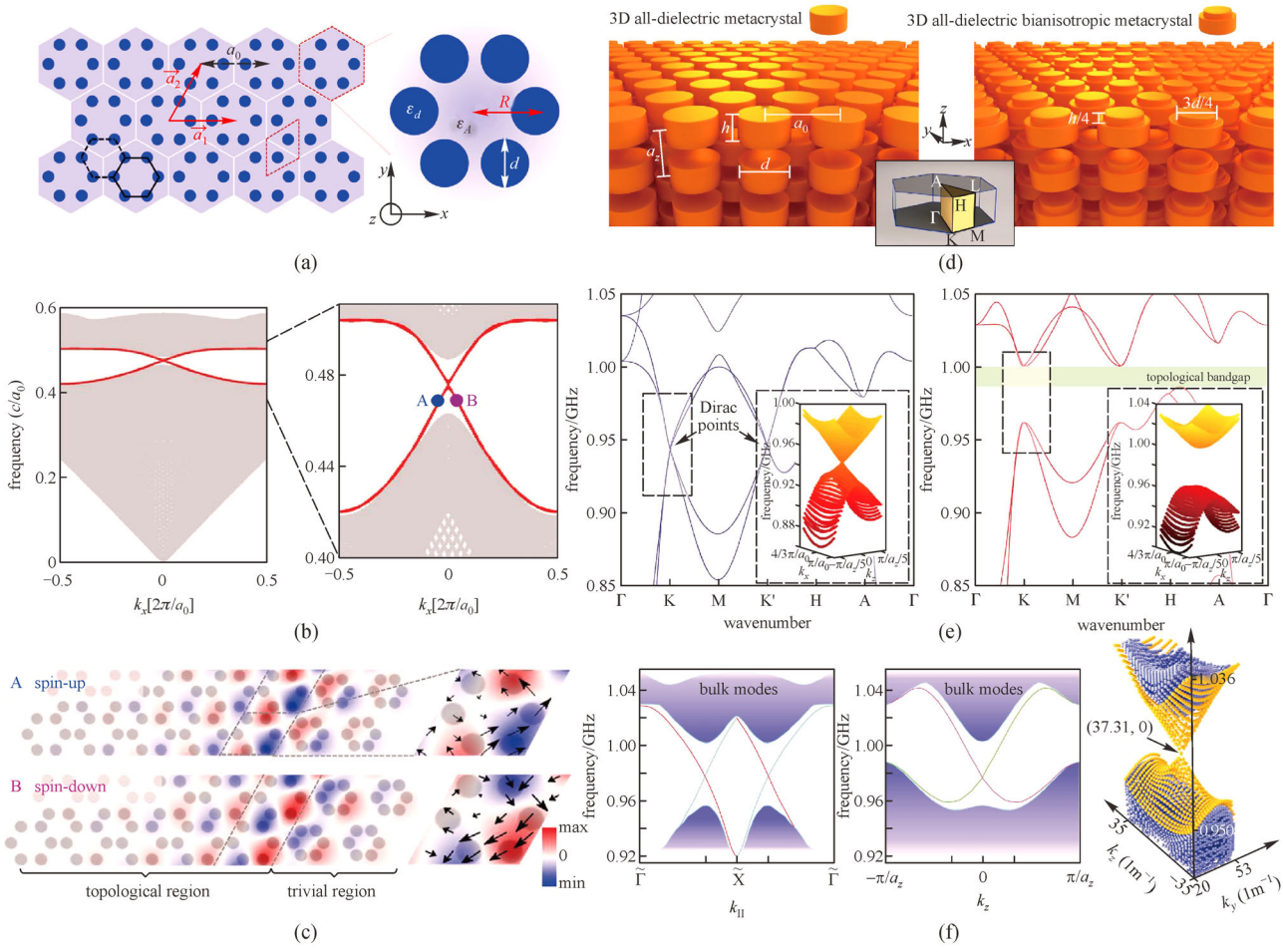

Fig. 3 (a) Schematic diagram of triangular photonic crystals; (b) projected dispersion of 2D topological photonic crystals; (c) electromagnetic field distributions (E_z) in different pseudospins; (d) schematics of the vertical domain composed of bianisotropic metacrystal; (e) band structures of two kinds of unit cells in (d); (f) dispersion relation of surface states with $k_{||}$ and $k_{\perp}$ directions. Reproduced from Refs. [21,37]

phases in gapless photonic crystals represent another important set of systems, characterized by Weyl points and nodal lines [126–128,130,131]. In three dimensions, Weyl points have a unique linear dispersion, which is in contrast to the Dirac points in 2D periodic systems. The Weyl Hamiltonian can be described by the following form

$$H(\boldsymbol{k}) = v_x k_x \sigma_x + v_y k_y \sigma_y + v_z k_z \sigma_z. \quad (7)$$

Here, $\boldsymbol{k} = (k_x, k_y, k_z)$ refers the three dimensional momentum space, and v_i are the group velocities.

When either P symmetry or T symmetry is broken, the nonzero Berry curvature is generated at Weyl points and causes the Chern number of ± 1. In addition to the degeneracy of the points, the degeneracy of the lines is also important in 3D systems. Such nodal lines can exist in PT symmetry with Berry phase π. The nodal systems that have been proposed so far include nodal rings, nodal links, nodal chains, and nodal knots. In 2013, a gyroid photonic crystal [130] is proposed to construct Weyl points and nodal lines by Lu et al, as shown in Fig. 4(a). Afterward, this idea is realized in the microwave frequencies [126]. Since then, several other similar ideas and experiments have come into light [127,128,131] (e.g., Fig. 4(b)).

3.2 Metallic photonic crystals

Usually, the metal acts as a wall to prevent waves from escaping in the direction other than the periodic structure. However, as a material, metals can also be applied in photonic crystals. Metal as a component of photonic crystals is mainly based on two properties. The first one is that the metal in the long-wavelength range can be regarded as a perfect electric conductor (PEC), such as microwave frequencies [22,137–139]. The other is to study the plasma characteristics using the Drude model, and the permittivity can be written as [140–143]

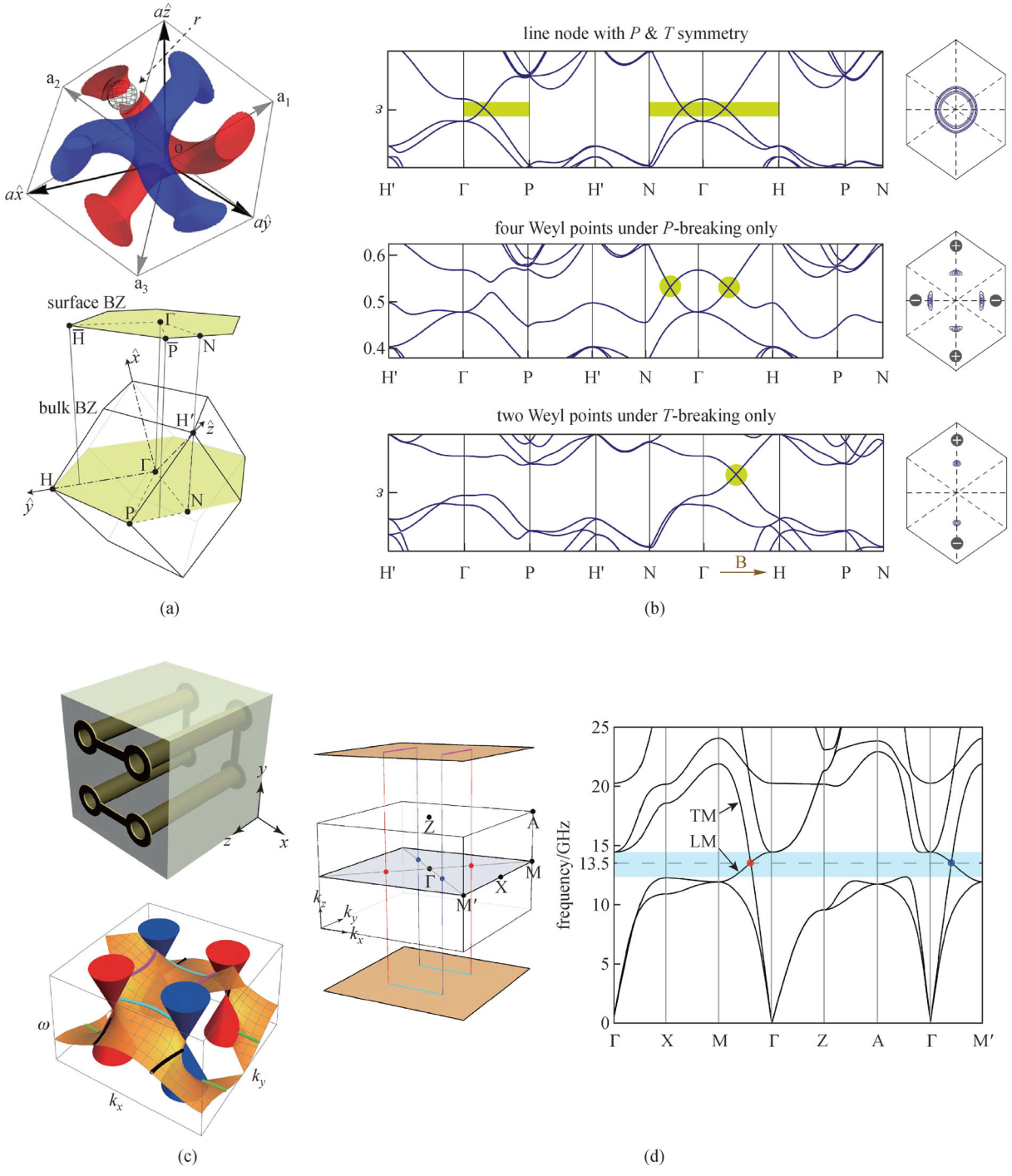

Fig. 4 (a) BCC unit cell of gyroid photonic crystals and corresponding Brillouin zone; (b) band structures of nodal lines with two air spheres on two gyroids; (c) schematic of metallic inclusion which includes the saddle shape, and helicoid surface states; (d) Brillouin zone of metallic inclusions and the band structures with Weyl points (rad/blue points). Reproduced from Refs. [130,131]

$$\varepsilon_r(\omega) = 1 - \frac{\omega_p^2}{\omega(\omega + \mathrm{i}\gamma)}. \tag{8}$$

Here, $\omega_p^2 = n_e e^2 / m\varepsilon_0$ is the plasma frequency, n_e is the number density of electrons and m means their effective mass. γ is the damping rate of plasma. In 2016, a simple structure was designed to achieve the quantum spin Hall effect of photonic crystals by Cheng et al. [22], considering the PEC properties of metals. Figures 5(a) and 5(b) show details of design and experimentation, carefully adjust the degeneracy of two pairs of Dirac cones for TE and TM modes, the pseudospin states are introduced to form a switch of topological edge states. In addition, Yang et al. reported a 3D topological photonic crystal [38] consisting

of metallic split-ring resonators (SRRs) in 2019. With the strong magneto-electric coupling, 3D Dirac points (with 4-fold degeneracy) tuned to breaking, and Dirac cone surface states have been observed experimentally at microwave frequencies. Valley Hall effects can also be realized in metal systems. In 2017, Wu et al. experimentally realized a valley Hall transport (surface plasmon) of edge states in the microwave regime [36]. Gao et al. experimentally demonstrated two pairs of robust kink states in valley photonic crystals by suspending a metallic tripod in a C_6 lattice [144]. The system of spoof surface plasmon polaritons with quantum valley Hall effects is also a good platform to create analogs of electrons [36]. In addition, the metal based on the Drude model is applied to study plasma topological edge states and gapless topological phases [140,142], and so on. As shown in Figs. 5(c) and 5(d), the nodal lines are observed in cut-wire metacrystals by Gao et al. [143] when the plasma dispersion of metal is introduced. Until recently, the photonic crystals based on metal are extensively studied due to their strong capabilities of the electromagnetic wave manipulation [22,137–143,145].

3.3 Optical resonator lattices

Optical resonators have a degree of freedom of transmission in two directions which can be equivalently described to a system with $1/2$ pseudospins. Due to the existence of two spins, the topological edge states are propagated in two opposite directions, which can be analogous to the quantum spin Hall effect. Optical resonators are usually described by tight binding models due to their coupling mechanism. For coupled-resonator optical waveguides (CROW) containing two sites in a unit structure (as shown in Fig. 6(a)), the Hamiltonian of the optical tight binding model can be expressed as [17]

$$H = -\kappa(\Sigma_{\sigma,x,y}\hat{a}^{\dagger}_{\sigma x+1,y}\hat{a}_{\sigma x,y}\mathrm{e}^{-\mathrm{i}2\pi\sigma y\sigma} + \hat{a}^{\dagger}_{\sigma x,y}\hat{a}_{\sigma x+1,y}\mathrm{e}^{\mathrm{i}2\pi\sigma y\sigma} + \hat{a}^{\dagger}_{\sigma x,y+1}\hat{a}_{\sigma x,y} + \hat{a}^{\dagger}_{\sigma x,y}\hat{a}_{\sigma x,y+1}). \tag{9}$$

Here, κ is the mode coupling rate of optical resonators, $\hat{a}^{\dagger}_{\sigma x,y}$ is the creation operator and $\hat{a}_{\sigma x,y}$ is the annihilation operator of photons at the site of the position (x,y) and the whole system has two opposite pseudospins $\sigma = \pm 1$. Chiral edge states also appear at the corresponding boundaries and are robust to the defects as shown in Fig. 6(b). The arrangement of the CROW changes when a single unit is consist of four site resonators [146] as shown in Fig. 6(d). Figure 6(c) shows that the topological edge states are insensitive to defects through the experimental platform of Fig. 6(a). Recent research shows that these optical resonators can also be used for the measurement of topological invariants [147], topological lasers [148,149] and non-Hermitian systems [65,150].

3.4 Coupled waveguide systems

A waveguide coupled along the direction of propagation (z) can be considered as a paraxial propagation system. One of the most common representative structures is depicted in Fig. 7(a), which is fabricated by the femtosecond laser writing method. Normally, the propagation of the paraxial light is described by [27]

$$\mathrm{i}\partial_z\psi(x,y,z) = -\frac{1}{2k_0}\nabla^2\psi(x,y,z) - \frac{k_0\Delta n(x,y,z)}{n_0}\psi(x,y,z). \tag{10}$$

Here, ψ is the envelope function of the electric field and $k_0 = 2\pi n_0/\lambda$ is the wavenumber of the ambient medium. Δn is the difference between the ambient medium and the waveguide medium. When waveguides become helical along the direction of propagation, the center of the waveguides changes on different cross sections. The positions translate into $x_h = x + R\cos(\Omega z)$, $y_h = y + R\sin(\Omega z)$ and $z_h = z$, here $\Omega = 2\pi/Z$ (Z is the period). In this case, the evolution of the light in helical waveguides transforms as [27]

$$\mathrm{i}\partial_{z_h}\psi_h = -\frac{1}{2k_0}(\nabla_h + \mathrm{i}A(z_h))^2\psi_h - \frac{k_0R^2\Omega^2}{2}\psi_h - \frac{k_0\Delta n(x_h,y_h)}{n_0}\psi_h. \tag{11}$$

Here, $A = k_0R\Omega[\sin(\Omega z_h),\cos(\Omega z_h),0]$ corresponds to a vector potential associated with the electric field of circular polarization. Band structures of Floquet edge states can be adjusted by R as seen in Fig. 7(b). It can also be seen from Figs. 7(c) and 7(d) that the topological edge states can still be transmitted with defects on the boundary.

There is another way to introduce equivalent time modulation. As shown in Fig. 7(e), four kinds of coupling $J_{1,2,3,4}$ appear periodically in the direction of propagation [30,31]. Similar to the helical waveguides, such a coupling produces chirality to form a Floquet Chern insulator. The propagation of edge states is shown in Fig. 7(f) for the emergence of chiral modes. Until now, optical coupling waveguide platforms are still widely used to study various physical problems, such as single-photon (or two-photon) transmission at topological edge states [151,152], non-Hermitian waveguides [66,72,77], etc.

3.5 Other proposals

In addition to the coupling mechanisms mentioned above, various new platforms for implementing coupling in photonic systems are being constantly explored. A typical example is a 2D array of monolithic distributed Bragg reflector (DBR) cavities [18], which is proposed by

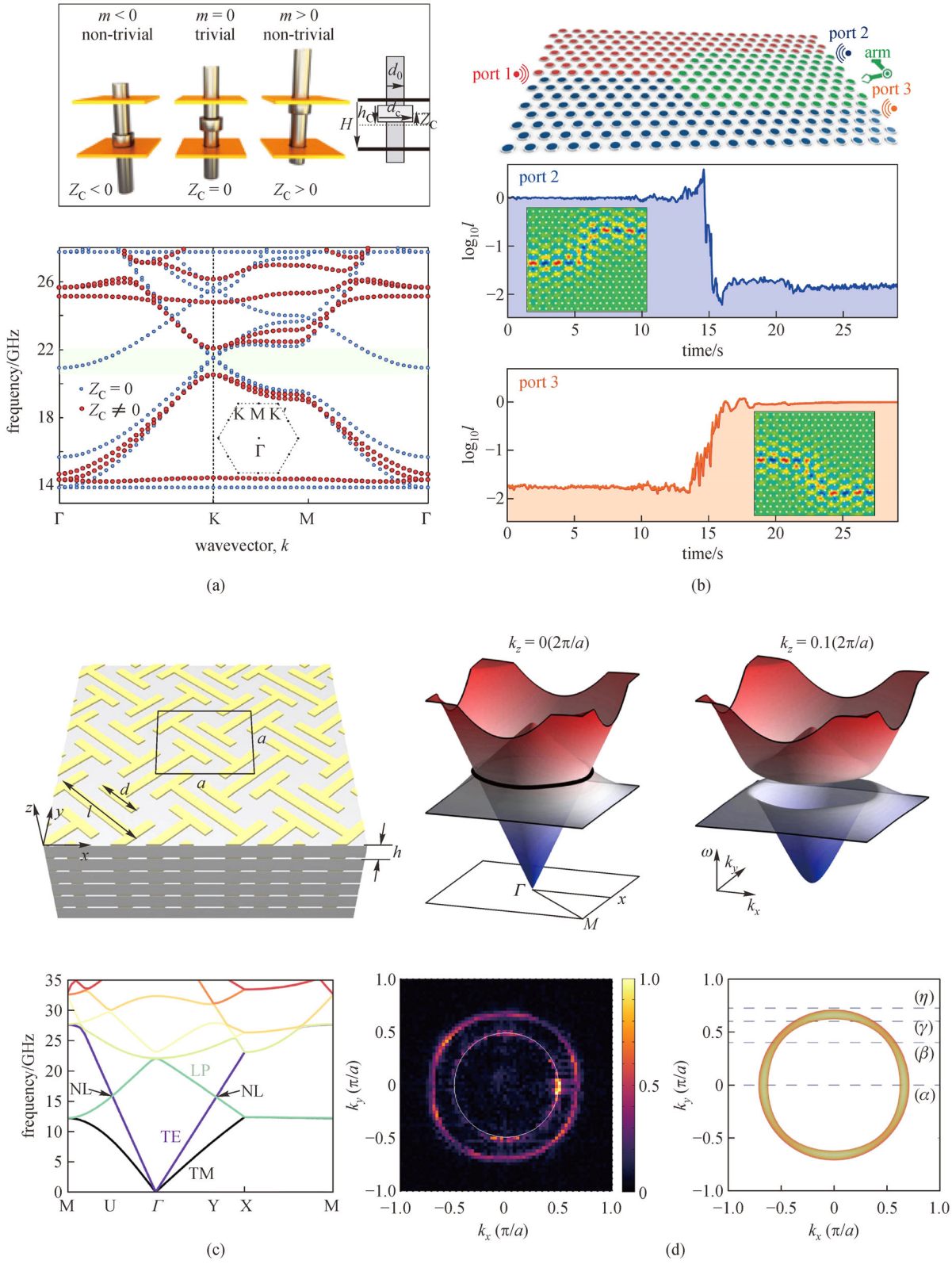

Fig. 5 (a) Arrangement of metallic rods and put into the parallel plate waveguide with different topology characteristics, and the corresponding band structures; (b) schematic plot of the topological switch and the transmission performance with switch operation; (c) schematic of metacrystals with copper cut-wire and their band structures; (d) band structures at $k_z = 0$ $(2\pi/a)$ and $k_z = 0.1$ $(2\pi/a)$ planes, and the measured result with the Fourier transform. Reproduced from Refs. [22,143]

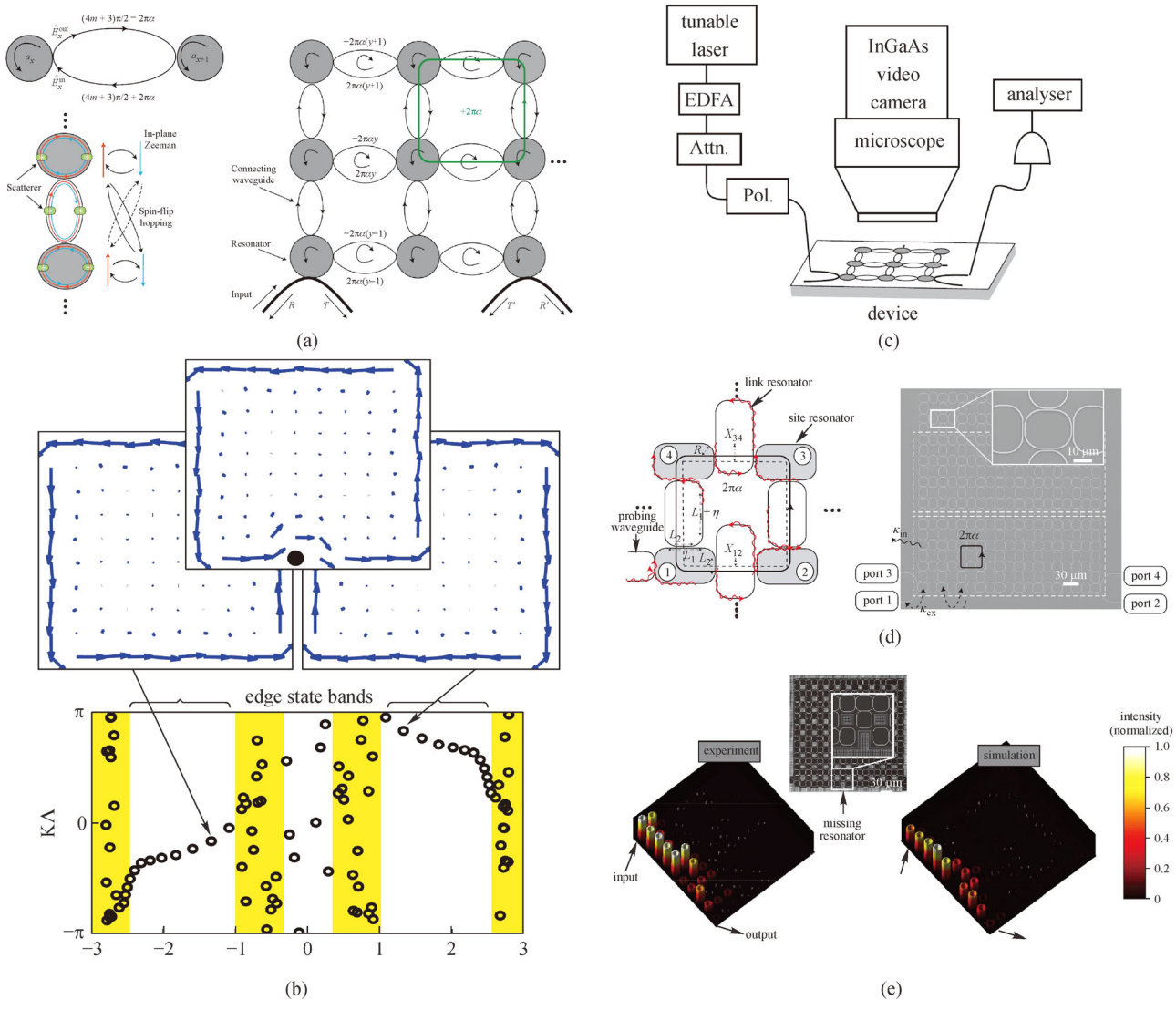

Fig. 6 (a) Two coupled resonators descripted by Hamiltonian with spin freedom and the 2D array of resonators; (b) edge states in different spins and the transmission in the presence of disorder perturbation; (c) experimental set-up for the measurement; (d) unit coupled resonators including four link and four site resonators, and the scanning electron microscope image (SEM) of the resonant array; (e) topological edge states that propagating around the defect in the experiment and simulation. Reproduced from Refs. [17,146]

Umucalılar and Carusotto in 2011. The cavities on sites contain an oblique mirror and are surrounded by DBR, while phase elements are placed between two cavities as shown in Figs. 8(a) and 8(b). This oblique mirror is used to lift the degeneracy of circularly polarized states $\sigma_{\pm}$. After the photons circle around the four cavities, the additional geometric phase is generated which is similar to the CROW.

Another type of proposal is based on the combination of novel material systems and classical photonic crystals. In particular, recently, some materials (e.g., graphene) have been demonstrated with many intriguing photonic properties such as optical absorption, nonlinear effect, plasma characteristics which enhance the integration of photonic crystals. Figure 8(c) shows the absorption properties of graphene in photonic crystals [153], which has the potential to introduce a non-Hermitian effect into traditional photonic crystals. Figures 8(d) and 8(e) show the light-matter interaction in graphene coupled to photonic crystals [154], which essentially reflects the advantages of having a composite system.

4 Exciting recent advances of photonic crystals

In recent times, the research prospects of topological photonic crystals continue to grow at a considerable rate.

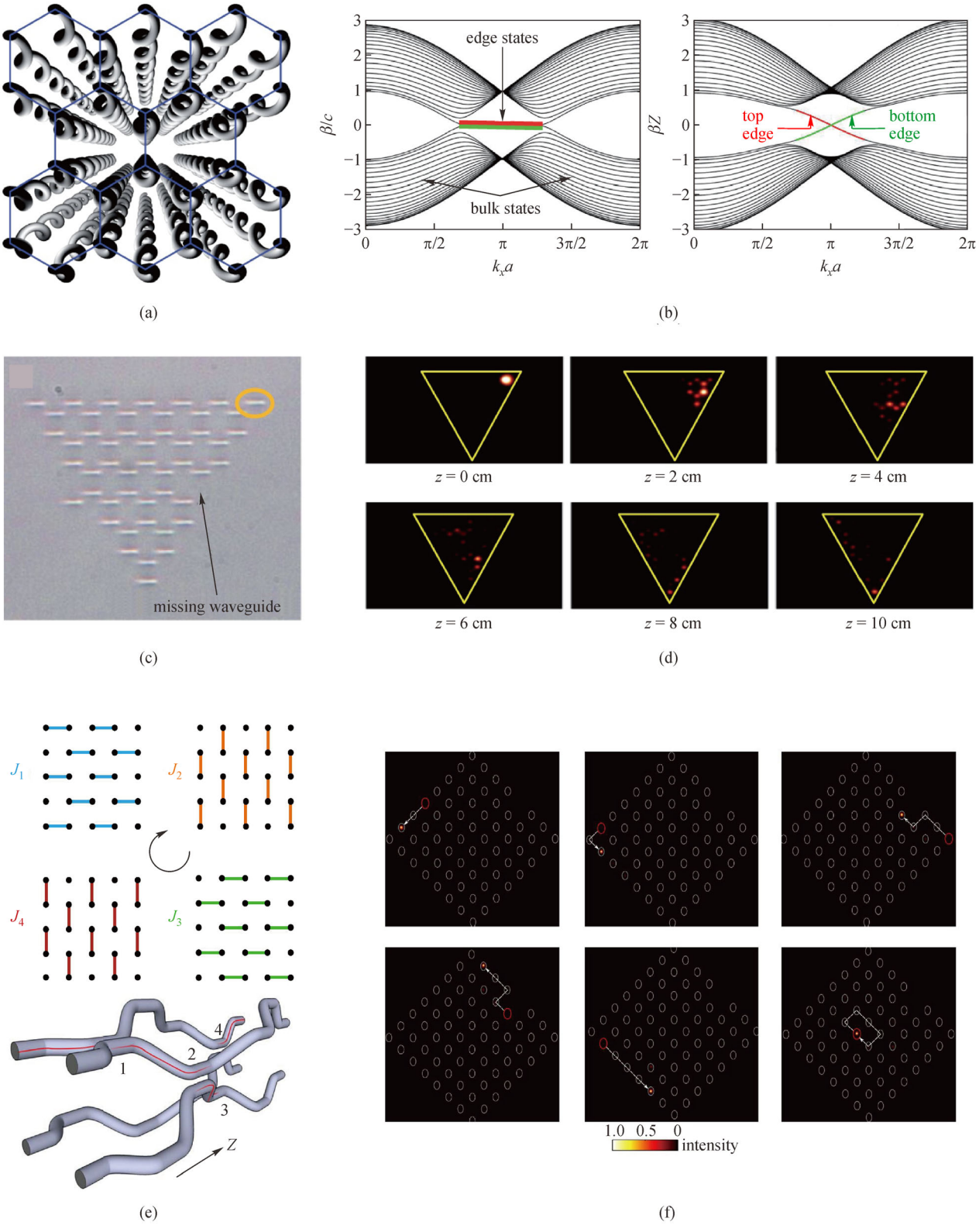

Fig. 7 (a) Schematics of the helical waveguides comprising the honeycomb lattice; (b) projected dispersion of straight waveguides ($R = 0$ μm) and helical waveguides ($R = 8$ μm); (c) microscope image of the photonic waveguide array; (d) light propagation at different distance, z means the length of distances; (e) four different bonds existed in the lattice with coupling constants $J_{1,2,3,4}$ and the sketch to achieve it; (f) experiment measured with chiral edge states along different paths. Reproduced from Refs. [27,31]

The synergy between optical and topological properties has unveiled the development of various new topics. In this section, we introduce the higher-order topological photonic crystal and nonlinear effects in photonic crystals, and non-Hermitian systems. Finally, other proposals are discussed in photonic crystals, such as topological insulator lasers, machine learnings for topological photonics, and Fano resonances.

4.1 Higher-order topological photonic crystals

The edge states without backscattering are the key feature of topological photonic insulators. Typically, the topological photonic insulators with n dimensions have the edge states of $n-1$ dimensions. Recent investigation indicates that some topological insulators have gapped states of $n-1$, $n-2$, $n-m-1$ dimensions while the last edge states are $n-m$ dimensional. Hence we call them mth-order topological photonic insulator [84–87, 91–97]. A second-order topological photonic is shown in Fig. 9(a), along similar lines of a 2D Su-Schrieffer-Heeger (SSH) model [155,156], this structure consists of two kinds of coupling which are achieved by adjusting the distance of column [94,95]. According to the tight binding model, the Hamiltonian of this system can be expressed as

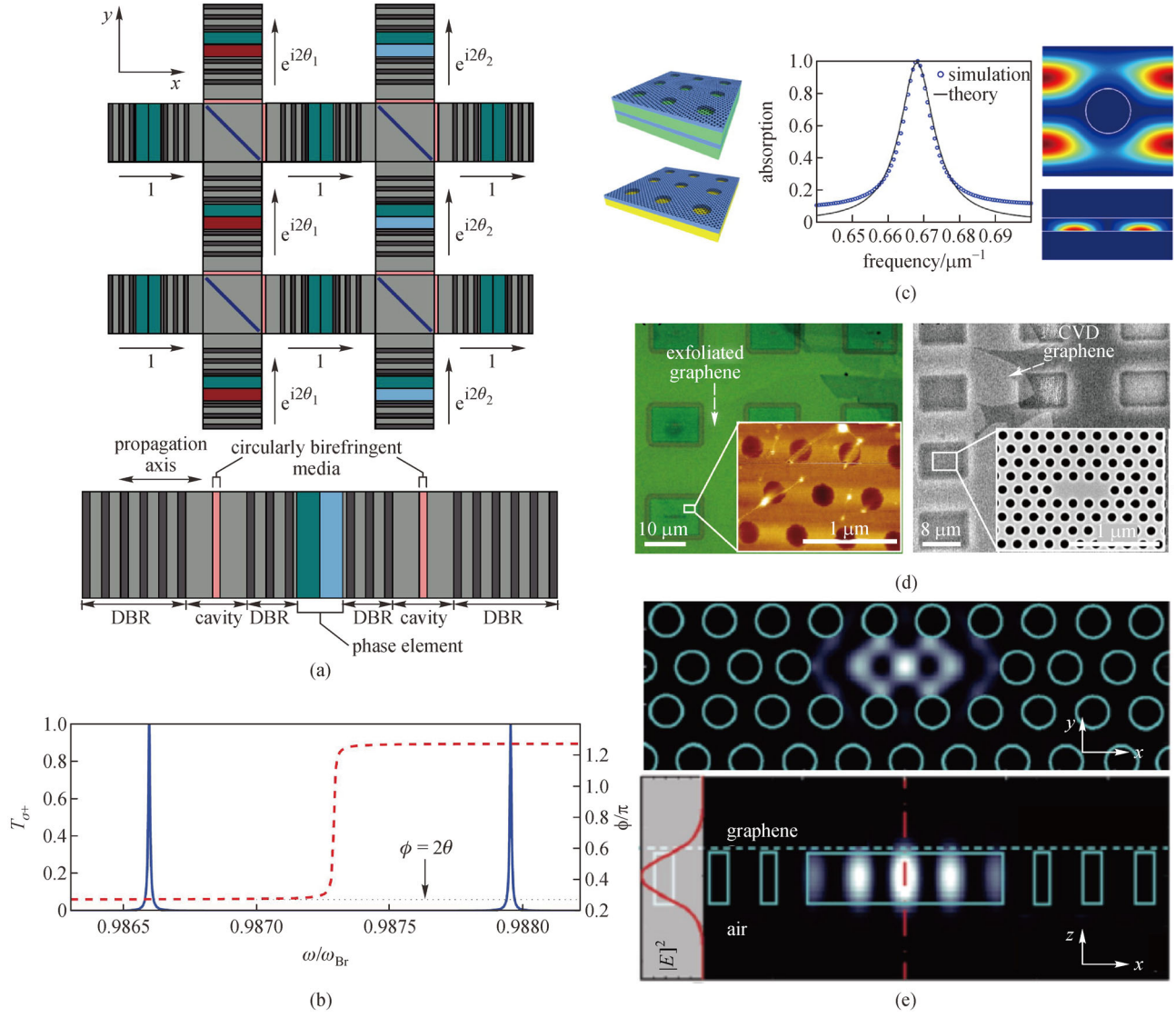

Fig. 8 (a) 2D square lattices made of DBR cavities and connected by phase elements; (b) transmission spectrum (blue line) of two cavities in (a) and the phase in two cavities (red dashed line); (c) schematic of a graphene layer combined with photonic crystals, and their absorption; (d) photonic crystals integrated with graphene. Their optical image of microscope and SEM image; (e) fundamental resonant mode of three-hole defect cavities. Reproduced from Refs. [18,153,154]

$$H(k)=\begin{pmatrix} 0 & h_{12} & h_{13} & 0 \\ h_{12}^{*} & 0 & 0 & h_{24} \\ h_{13}^{*} & 0 & 0 & h_{34} \\ 0 & h_{24}^{*} & h_{34}^{*} & 0 \end{pmatrix}, \qquad (12)$$

where, $h_{34}=h_{12}=t_a+t_b\exp(\mathrm{i}k_x a)$, $h_{24}=h_{13}=t_a+t_b\exp(-\mathrm{i}k_y a)$, t_a and t_b correspond to the internal coupling and the coupling between units, a is the lattice constant. Figure 9(b) shows the process of opening-closing-opening of the band structure. Here, a 2D Zak phase can be proposed to describe this system.

$$P_i=-\frac{1}{(2\pi)^2}\int_{\mathrm{BZ}} \mathrm{d}^2\boldsymbol{k}\mathrm{Tr}\left[\hat{A}_i\right], \qquad i=x,y. \qquad (13)$$

Here, $\hat{A}_i(\boldsymbol{k})=i\langle\psi_m(\boldsymbol{k})|\partial_{k_i}|\psi_n(\boldsymbol{k})\rangle$, and m, n refer to the eigenvectors of the mth, nth bands. For trivial case, the Zak phase $P=(P_x,P_y)=(0,0)$, and nontrivial case $P=(1/2,1/2)$. Figures 9(c), 9(d) and 9(e) show the real structure and the eigenvalues of bulk, edge, and corner states. Simulation and experiment show that this system not only has 1D edge states but also 0D corner states as seen in Figs. 9(f) and 9(g), which reveals the potential of higher-order topological insulators for dimensional manipulation of topological phenomena. More extensive research is also being carried out in microwave quadruple insulator [91], photonic crystal nanocavity [96], breathing kagome and pyrochlore lattice [84,87].

4.2 Photonic crystals with nonlinear effects

Unlike previous linear systems described by Maxwell's equation in linear dielectric and magnetic permittivity, novel features of a topological system with nonlinear photonic effects such as Kerr nonlinear effects and strong photonic interactions [26,47–60], are highlighted in this part. When the SSH chain model introduces nonlinear effects such as the Kerr-like nonlinear effect as shown in Fig. 10(a), the nonlinear Schrödinger equation can be written as [54]

$$\mathrm{i}\frac{\psi_n}{\mathrm{d}t}=\Omega\psi_n+\boldsymbol{K}_m(n)\psi_{n-1}+\boldsymbol{K}_p(n)\psi_{n+1}. \qquad (14)$$

Here $\Omega=(\omega_0,v;\ v,\omega_0)$ and ω_0,v signifies the on-site resonance frequency and coupling coefficients of the interior of a unit cell. $\boldsymbol{K}_m(n)=[0,\ k_0+\alpha(|a_{1,n}|^2+|a_{2,n-1}|^2);0,0]$ and $\boldsymbol{K}_p(n)=[0,0;\ k_0+\alpha(|a_{1,n+1}|^2+|a_{2,n}|^2),0]$ where k_0 is the linear term ($k_0>0$) and α is the Kerr-like coefficient ($\alpha\geqslant 0$). Figure 10(b) shows the gapped band structure of trivial case with winding number $W=0$, when the intensity $I=0$. Figures 10(c) and 10(d) show the change of band structure and winding number with intensity, which confirms the fact that the intensity-dependent nonlinear effects can lead to topological phase transitions.

Using the interplay of particle interactions, external fields, and spatial symmetries, the rotation of photons in one direction indicates the breaking of TRS [56] as shown in Figs. 10(e) and 10(f). Noninteracting photons rotate like single photons and the direction is determined by synthetic magnetic fields. For strong photonic interactions, the path of photon vacancies appears in the opposite direction. In addition, topological aspects of nonlinear photonic crystals are constantly being explored such as nonlinear Floquet systems [26,55], nonlinear control of edge states [59] and interacting Harper–Hofstadter model [57].

4.3 Non-Hermitian photonic crystals

Photonic crystals with gain and loss have known to possess exotic non-Hermitian topological effects, both fundamentally and in respective their applications. The bulk-boundary correspondence [70] and symmetries (especially PT symmetry) [73] are the two of the most active lines in non-Hermitian systems. The unique features imposed by non-Hermiticity is the exceptional point (EP). First, let's examine the situation of a single EP, which is essentially the non-Hermitian degeneracy point in parameter space. Notably, it is also the point at which PT symmetry is spontaneously broken and eigenspace collapses [157,158]. Consider a case for which a pair of exceptional points merge into a Dirac point, and the non-Hermitian Hamiltonian is given by [79]

$$H=(k_x+\mathrm{i}\delta)\sigma_x+k_y\sigma_y. \qquad (15)$$

Here, two EPs appear at $k=(0,\pm\delta)$, as $\delta\rightarrow 0$, the EPs translate into the Dirac point. In addition, the vorticity of band structures can be defined as

$$v_{mn}=-\frac{1}{2\pi}\oint_{\Gamma}\nabla_k Arg(E_m(k)-E_n(k))\cdot\mathrm{d}k. \qquad (16)$$

Here, Γ is a loop of momentum space, E_m and E_n are the eigenfrequencies of m,n bands. The vorticity of each EP is $\pm 1/2$ respectively as shown in Fig. 11(a).

The other situation is slightly different, for the onsite gain or loss, the Hamiltonian of Dirac dispersive can be rewritten as [67]

$$H=\begin{pmatrix} \mathrm{i}\gamma & v_D(k_x-\mathrm{i}k_y) \\ v_D(k_x+\mathrm{i}k_y) & -\mathrm{i}\gamma \end{pmatrix}. \qquad (17)$$

Here, v_D is the group velocity, and γ signifies the offset of gain and loss. The complex eigenvalues $E_{\pm}=\sqrt{v_D(k_x^2+k_y^2)-\gamma^2}$, which refer to the ring of EP appeared when $\boldsymbol{k}$ satisfies the condition $v_D(k_x^2+k_y^2)=\gamma^2$.

For experiments, the waveguide array system can satisfactorily achieve this effect in the 1D situation as shown in Fig. 11(b). The topological edge state in PT symmetric system has been experimentally demonstrated

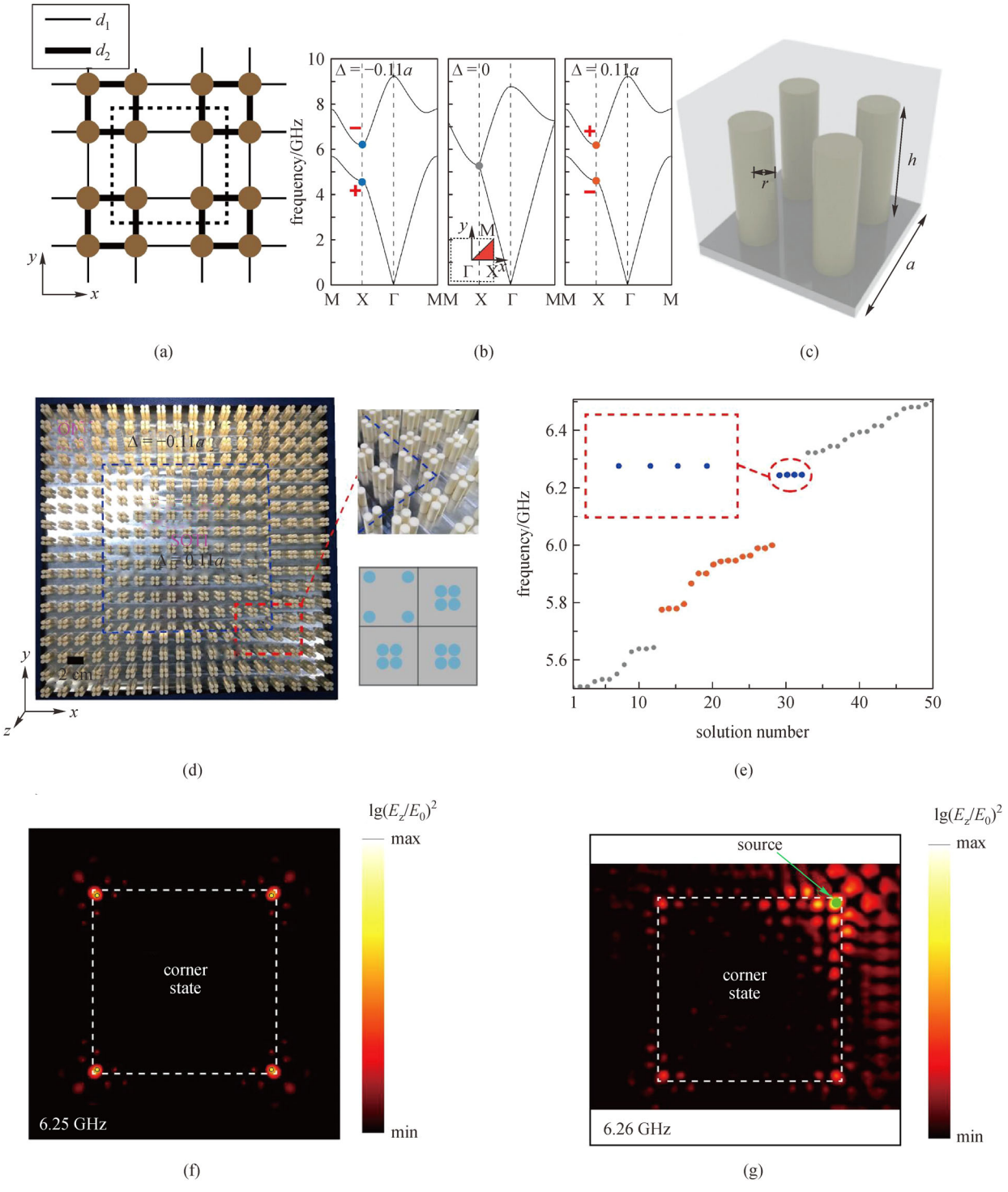

Fig. 9 (a) 2D lattice of photonic crystal, where d1 and d2 corresponding to the coupling expressed in distance; (b) band structures of trivial, gapless, and nontrivial situations; (c) diagram of 3D structure; (d) photograph of higher-order topological insulator surrounded by ordinary insulators; (e) eigenfrequencies of bulk, edge and corner states; (f) simulation of corner states; (g) experimental measurement of the corner states. Reproduced from Ref. [95]

by Weimann et al. in 2017 [72]. Photonic crystals slabs provide a radiation-induced platform for a 2D situation due to the non-Hermiticity-induced form radiation. As shown in Fig. 11(c), the SEM image and experimental results

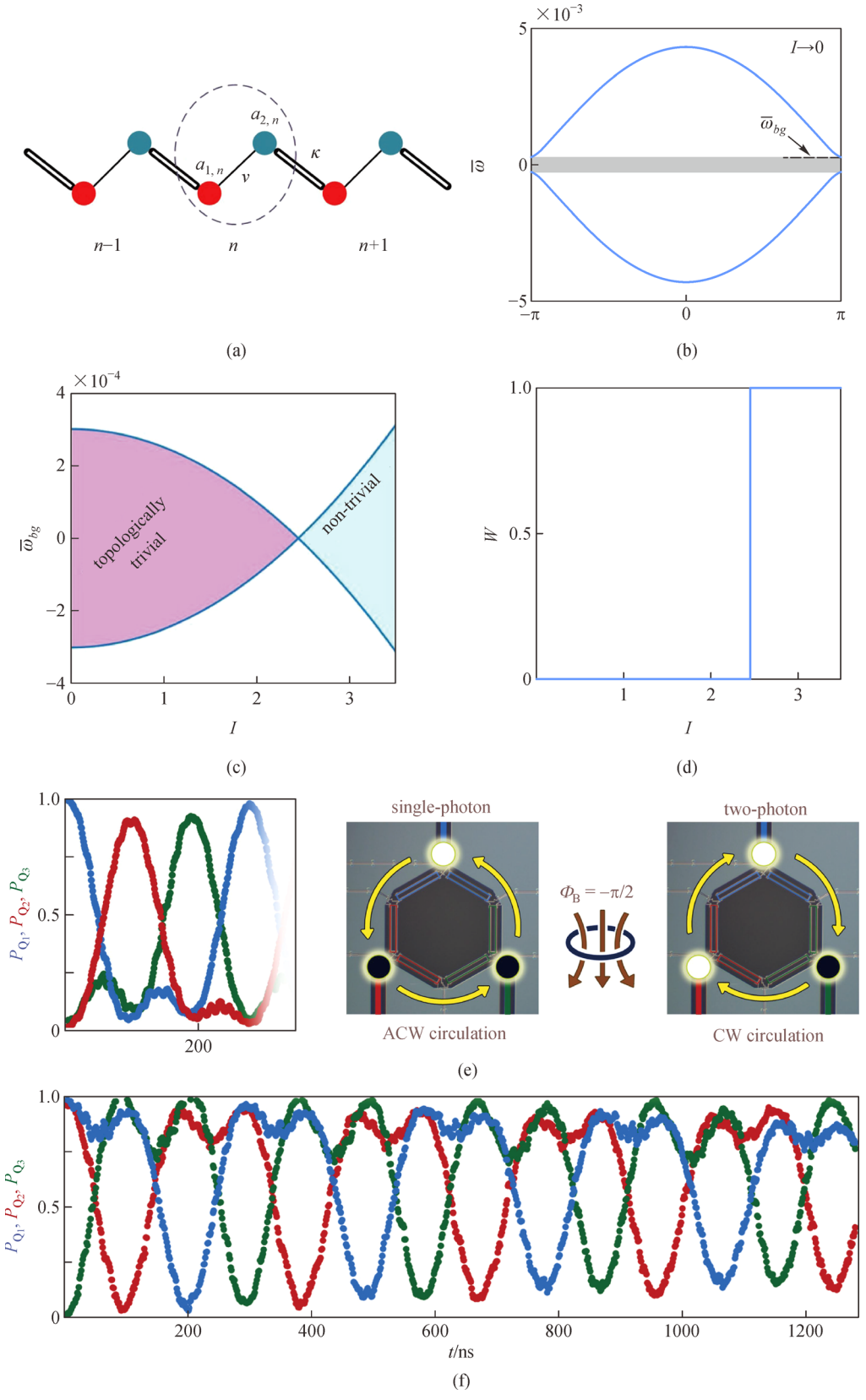

Fig. 10 (a) Nonlinear SSH model, two resonators in every unit cell; (b) band structures of trivial case when the mode intensity $I = 0$; (c) width of band gap changed by intensity; (d) winding number tuned by intensity; (e) time evolution of excitation probability for single-photon state in three qubits $Q_{1,2,3}$; (f) probability for a two-photon case. Reproduced from Refs. [54,56]

indicate that this system can be described by the Hamiltonian we discussed above [67].

The bulk-boundary correspondence of non-Hermitian systems also encountered challenges in the following three respects. One is how to define a gap for complex band structures, Shen et al. [79] provide the proposals to define "separable," "isolated" and "inseparable" by their eigenvalues $E_n(\boldsymbol{k}) \neq E_m(\boldsymbol{k})$, $E_n(\boldsymbol{k}) \neq E_m(\boldsymbol{k}')$ and $E_n(\boldsymbol{k}) = E_m(\boldsymbol{k})$, where $n \neq m$. The second one is the extreme sensitive relationships of the band structure to boundary conditions [159]. The third one is all eigenstates may be localized at the boundary for an ordered non-Hermitian lattice [159]. In addition to the above-mentioned works, recently there has been a great deal of interest in different systems and models such as non-Hermitian SSH models [72,76], non-Hermitian Chern bands [81], and zero modes in a non-Hermitian system [77]. Topology and different symmetry paradigms can yield interesting effects in the non-Hermitian topological setting [160].

4.4 Other proposals

For a long time, besides the exciting possibilities in topological physics, researchers have also been exploring applications of topological photonic crystals. Topological insulator lasers have recently been proposed as highly efficient lasers, robust to disorders and defects. The topological insulator laser of 1D periodic systems mainly built on the SSH model [155,156] using coupled micropillars [161] or microing resonators [162]. In 2017, St-Jean et al. reported the lasing of topological edge states in zigzag chains of coupled semiconductor micropillars [161]. The topological edges states present a nonzero Zak phase and the robustness of against lattice deformations. Interestingly, the $p_{x,y}$ modes participate in this topological model and lead to the edge states of p orbitals. In 2018, Zhao et al. proposed to introduce the non-Hermitian mechanism in SSH models to realize zero modes, which are suitable for integrated silicon photonics [163]. Besides, the topological lasing in the microing resonators [162] and nanocavities [164] has also been proved experimentally. For a 2D periodic system, recently, Harari et al. [148] proposed a 2D topological insulator laser based on the Haldane model [165], where the dynamics is described by the real coupling between nearest neighbors, and the complex coupling between next-nearest neighbors opens a bandgap at the Dirac points. By introducing gain characteristics at the boundary, semiconductor lasers support single-mode and high-power transport without magnetic fields. In the same year, Bandres et al. first demonstrated this lasing phenomenon experimentally [149].

Machine learnings, as one of the most exciting science tools, have proved to effectively work on both physics and applications for topological photonics [166]. Recently, the machine learning for 1D topological photonic crystals shows the potential of this technique. In 2018, Pilozzi et al. [167] trained an artificial neural network (ANN) for the Aubry-Andre-Harper band structure. Using this ANN, topologically protected edge states at the target frequency can be obtained by identifying parameters of 1D topological insulators. In 2019, Long et al. focused on the correlation between Zak phases of 1D photonic crystals and space parameters by machine learnings. By determining the Zak phase property, band structures of the system can be determined, which present a bright future for the inverse design of topological photonic crystals [168]. For higher-dimensional photonic crystal, recently, Barth and Becker presented a method by combining the light field in 2D photonic crystals and classification of photonic modes. Large amounts of data collected by numerical simulations or experiments are clustered and identified into different spatial properties by machine learnings [169].

Fano resonances [170] occur when discrete quantum states interfere with states of the continuum spectrum with a sharp asymmetric transmission, showing the potential application in sensing and switching of photonic crystals [171–173]. Until recently, Fano resonances in topological photonic crystals present a high quality and topologically protected cavity [174,175]. In 2018, Gao et al. combined the topological edge states and Fano resonances, experimentally produced a high-quality ($Q \approx 10^4$) resonance in optical communication ranges [174]. In 2019, Zangeneh-Nejad and Fleury induced the concept of topological Fano resonances and demonstrated that the ultrasharp spectrum for Fano resonances robustness to the geometrical disorder [175]. They claimed that, as a general property of waves, topological Fano resonances can also be found in plasmonic, optical, and microwave systems.

5 Conclusions

In summary, we have presented a brief review of the recent achievements in the area of topological photonic crystals. In analogy with topological phenomena in condensed matter physics, its photonic analog has received increased attention due to many unique advantages reminiscent of photonics, such as controllable photons interactions [57], rich varieties of the coupling mechanism [127,132,137, 154,176], and versatile experimental settings [24,31,125, 126,132,133,143]. In addition, since it is rooted in the photonic system, topological photonic crystals can also take advantage of optical effects such as nonlinear optical effects [31,47,48,50,52,53,55,59,100,101,112,133], gain or loss systems [62,67,69,77,78,91,142], optical propagation systems [26,27,30,33,34,98], anisotropic (or bianisotropic) materials [132,133], and quantum optics [57,110]. The results are promising not only in fundamental understanding pertaining to these fields but also numerous

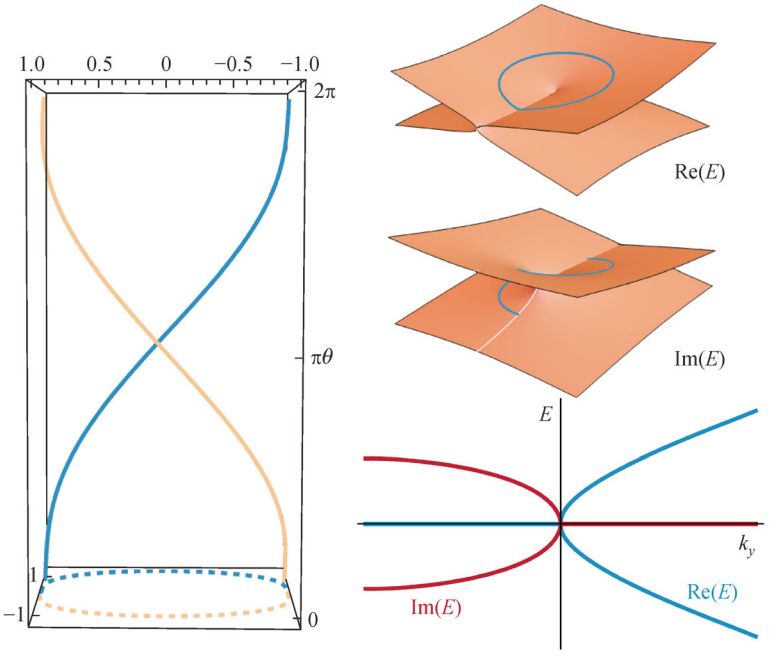

(a)

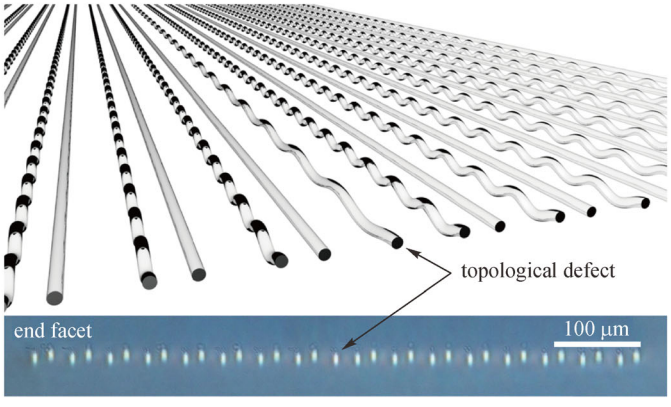

(b)

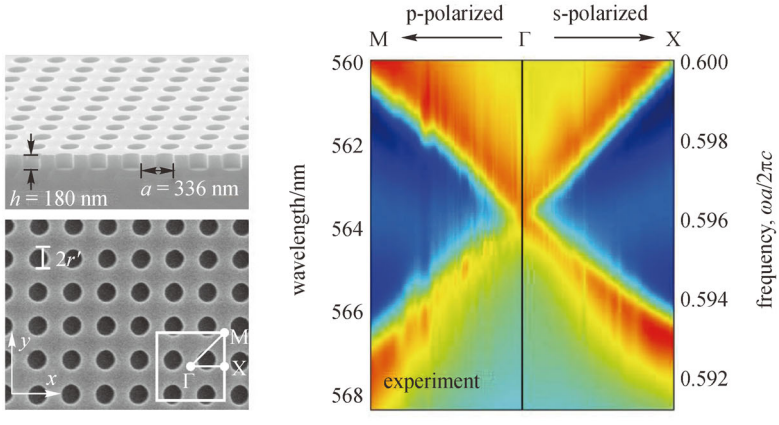

(c)

Fig. 11 (a) Dispersion of non-Hermitian system near the exceptional points; (b) array of passive waveguides and realized structure of fused silica glass; (c) SEM image of photonic crystal slabs and their band structure measured by experiment. Reproduced from Refs. [67,72,79]

optical applications such as topologically protected edge states without backscattering [15,31,74,82,137,146], topological lasers [148,149], and topological waveguides [14,24,132].

In future, many active directions of research could find important ramifications, such as: integrated and tunable robust transports, which play an important role in the promotion of topological devices; topological active devices such as integrated topological lasers and quantum sources, which can widen the scope of quantum communication and quantum optics; direct measurements of topological phases which can play an important role in the display of topological information of photonic crystals. It can be anticipated that with the continuous developments of topological phases of matter in new directions with intriguing physical effects at one hand and an equally complementary micro- and nanofabrication technology on the other, topological photonic crystals will find increasing scientific interests.

Acknowledgements This work was supported by the National Key R&D Program of China (Nos. 2018YFA0306200, and 2017YFA0303702) and the National Natural Science Foundation of China (Grant Nos. 11625418, 51732006, and 11890700), as well as the Academic Program Development of Jiangsu Higher Education (PAPD).

References

1. Yablonovitch E. Inhibited spontaneous emission in solid-state physics and electronics. Physical Review Letters, 1987, 58(20): 2059–2062
2. John S. Strong localization of photons in certain disordered dielectric superlattices. Physical Review Letters, 1987, 58(23): 2486–2489
3. Wang B, Cappelli M A. A plasma photonic crystal bandgap device. Applied Physics Letters, 2016, 108(16): 161101
4. Akahane Y, Asano T, Song B S, Noda S. High-Q photonic nanocavity in a two-dimensional photonic crystal. Nature, 2003, 425(6961): 944–947
5. Shelby R A, Smith D R, Schultz S. Experimental verification of a negative index of refraction. Science, 2001, 292(5514): 77–79
6. Shalaev V M, Cai W, Chettiar U K, Yuan H K, Sarychev A K, Drachev V P, Kildishev A V. Negative index of refraction in optical metamaterials. Optics Letters, 2005, 30(24): 3356–3358
7. Klitzing K, Dorda G, Pepper M. New method for high-accuracy determination of the fine-structure constant based on quantized hall resistance. Physical Review Letters, 1980, 45(6): 494–497
8. Thouless D J, Kohmoto M, Nightingale M P, den Nijs M. Quantized hall conductance in a two-dimensional periodic potential. Physical Review Letters, 1982, 49(6): 405–408
9. Kohmoto M. Topological invariant and the quantization of the Hall conductance. Annals of Physics, 1985, 160(2): 343–354
10. Kane C L, Mele E J. Quantum spin Hall effect in graphene. Physical Review Letters, 2005, 95(22): 226801
11. Bernevig B A, Zhang S C. Quantum spin Hall effect. Physical Review Letters, 2006, 96(10): 106802
12. Bernevig B A, Hughes T L, Zhang S C. Quantum spin Hall effect and topological phase transition in HgTe quantum wells. Science, 2006, 314(5806): 1757–1761
13. König M, Wiedmann S, Brüne C, Roth A, Buhmann H, Molenkamp L W, Qi X L, Zhang S C. Quantum spin hall insulator state in HgTe quantum wells. Science, 2007, 318(5851): 766–770
14. Haldane F D, Raghu S. Possible realization of directional optical waveguides in photonic crystals with broken time-reversal symmetry. Physical Review Letters, 2008, 100(1): 013904
15. Wang Z, Chong Y D, Joannopoulos J D, Soljacić M. Reflection-free one-way edge modes in a gyromagnetic photonic crystal. Physical Review Letters, 2008, 100(1): 013905
16. Wang Z, Chong Y, Joannopoulos J D, Soljacić M. Observation of unidirectional backscattering-immune topological electromagnetic states. Nature, 2009, 461(7265): 772–775
17. Hafezi M, Demler E A, Lukin M D, Taylor J M. Robust optical delay lines with topological protection. Nature Physics, 2011, 7(11): 907–912
18. Umucalılar R O, Carusotto I. Artificial gauge field for photons in coupled cavity arrays. Physical Review A, 2011, 84(4): 043804
19. Khanikaev A B, Mousavi S H, Tse W K, Kargarian M, MacDonald A H, Shvets G. Photonic topological insulators. Nature Materials, 2013, 12(3): 233–239
20. Nalitov A V, Malpuech G, Terças H, Solnyshkov D D. Spin-orbit coupling and the optical spin Hall effect in photonic graphene. Physical Review Letters, 2015, 114(2): 026803
21. Wu L H, Hu X. Scheme for achieving a topological photonic crystal by using dielectric material. Physical Review Letters, 2015, 114(22): 223901
22. Cheng X, Jouvaud C, Ni X, Mousavi S H, Genack A Z, Khanikaev A B. Robust reconfigurable electromagnetic pathways within a photonic topological insulator. Nature Materials, 2016, 15(5): 542–548
23. Dong J W, Chen X D, Zhu H, Wang Y, Zhang X. Valley photonic crystals for control of spin and topology. Nature Materials, 2017, 16(3): 298–302
24. Yang Y, Xu Y F, Xu T, Wang H X, Jiang J H, Hu X, Hang Z H. Visualization of a unidirectional electromagnetic waveguide using topological photonic crystals made of dielectric materials. Physical Review Letters, 2018, 120(21): 217401
25. Fang K, Yu Z, Fan S. Realizing effective magnetic field for photons by controlling the phase of dynamic modulation. Nature Photonics, 2012, 6(11): 782–787
26. Lumer Y, Plotnik Y, Rechtsman M C, Segev M. Self-localized states in photonic topological insulators. Physical Review Letters, 2013, 111(24): 243905
27. Rechtsman M C, Zeuner J M, Plotnik Y, Lumer Y, Podolsky D, Dreisow F, Nolte S, Segev M, Szameit A. Photonic Floquet topological insulators. Nature, 2013, 496(7444): 196–200
28. Titum P, Lindner N H, Rechtsman M C, Refael G. Disorder-induced Floquet topological insulators. Physical Review Letters, 2015, 114(5): 056801
29. Leykam D, Rechtsman M C, Chong Y D. Anomalous topological phases and unpaired dirac cones in photonic Floquet topological insulators. Physical Review Letters, 2016, 117(1): 013902

30. Maczewsky L J, Zeuner J M, Nolte S, Szameit A. Observation of photonic anomalous Floquet topological insulators. Nature Communications, 2017, 8(1): 13756
31. Mukherjee S, Spracklen A, Valiente M, Andersson E, Öhberg P, Goldman N, Thomson R R. Experimental observation of anomalous topological edge modes in a slowly driven photonic lattice. Nature Communications, 2017, 8(1): 13918
32. Mukherjee S, Chandrasekharan H K, Öhberg P, Goldman N, Thomson R R. State-recycling and time-resolved imaging in topological photonic lattices. Nature Communications, 2018, 9(1): 4209
33. Zhu B, Zhong H, Ke Y, Qin X, Sukhorukov A A, Kivshar Y S, Lee C. Topological Floquet edge states in periodically curved waveguides. Physical Review A, 2018, 98(1): 013855
34. Nathan F, Abanin D, Berg E, Lindner N H, Rudner M S. Anomalous Floquet insulators. Physical Review B, 2019, 99(19): 195133
35. Ma T, Shvets G. All-Si valley-Hall photonic topological insulator. New Journal of Physics, 2016, 18(2): 025012
36. Wu X, Meng Y, Tian J, Huang Y, Xiang H, Han D, Wen W. Direct observation of valley-polarized topological edge states in designer surface plasmon crystals. Nature Communications, 2017, 8(1): 1304
37. Slobozhanyuk A, Mousavi S H, Ni X, Smirnova D, Kivshar Y S, Khanikaev A B. Three-dimensional all-dielectric photonic topological insulator. Nature Photonics, 2017, 11(2): 130–136
38. Yang Y, Gao Z, Xue H, Zhang L, He M, Yang Z, Singh R, Chong Y, Zhang B, Chen H. Realization of a three-dimensional photonic topological insulator. Nature, 2019, 565(7741): 622–626
39. Young S M, Zaheer S, Teo J C, Kane C L, Mele E J, Rappe A M. Dirac semimetal in three dimensions. Physical Review Letters, 2012, 108(14): 140405
40. Yang B J, Nagaosa N. Classification of stable three-dimensional Dirac semimetals with nontrivial topology. Nature Communications, 2014, 5(1): 4898
41. Liu Z K, Zhou B, Zhang Y, Wang Z J, Weng H M, Prabhakaran D, Mo S K, Shen Z X, Fang Z, Dai X, Hussain Z, Chen Y L. Discovery of a three-dimensional topological Dirac semimetal, Na3Bi. Science, 2014, 343(6173): 864–867
42. Yang B, Guo Q, Tremain B, Barr L E, Gao W, Liu H, Béri B, Xiang Y, Fan D, Hibbins A P, Zhang S. Direct observation of topological surface-state arcs in photonic metamaterials. Nature Communications, 2017, 8(1): 97
43. Li F, Huang X, Lu J, Ma J, Liu Z. Weyl points and Fermi arcs in a chiral phononic crystal. Nature Physics, 2018, 14(1): 30–34
44. Burkov A A, Hook M D, Balents L. Topological nodal semimetals. Physical Review B, 2011, 84(23): 235126
45. Yan Z, Wang Z. Tunable Weyl points in periodically driven nodal line semimetals. Physical Review Letters, 2016, 117(8): 087402
46. He H, Qiu C, Ye L, Cai X, Fan X, Ke M, Zhang F, Liu Z. Topological negative refraction of surface acoustic waves in a Weyl phononic crystal. Nature, 2018, 560(7716): 61–64
47. Adair R, Chase L L, Payne S A. Nonlinear refractive index of optical crystals. Physical Review B, 1989, 39(5): 3337–3350
48. Berger V. Nonlinear photonic crystals. Physical Review Letters, 1998, 81(19): 4136–4139
49. Mingaleev S F, Kivshar Y S. Self-trapping and stable localized modes in nonlinear photonic crystals. Physical Review Letters, 2001, 86(24): 5474–5477
50. Soljačić M, Luo C, Joannopoulos J D, Fan S. Nonlinear photonic crystal microdevices for optical integration. Optics Letters, 2003, 28(8): 637–639
51. Fleischer J W, Segev M, Efremidis N K, Christodoulides D N. Observation of two-dimensional discrete solitons in optically induced nonlinear photonic lattices. Nature, 2003, 422(6928): 147–150
52. Soljačić M, Joannopoulos J D. Enhancement of nonlinear effects using photonic crystals. Nature Materials, 2004, 3(4): 211–219
53. Haddad L H, Weaver C M, Carr L D. The nonlinear Dirac equation in Bose–Einstein condensates: I. Relativistic solitons in armchair nanoribbon optical lattices. New Journal of Physics, 2015, 17(6): 063033
54. Hadad Y, Khanikaev A B, Alù A. Self-induced topological transitions and edge states supported by nonlinear staggered potentials. Physical Review B, 2016, 93(15): 155112
55. Leykam D, Chong Y D. Edge solitons in nonlinear-photonic topological insulators. Physical Review Letters, 2016, 117(14): 143901
56. Roushan P, Neill C, Megrant A, Chen Y, Babbush R, Barends R, Campbell B, Chen Z, Chiaro B, Dunsworth A, Fowler A, Jeffrey E, Kelly J, Lucero E, Mutus J, O'Malley P J J, Neeley M, Quintana C, Sank D, Vainsencher A, Wenner J, White T, Kapit E, Neven H, Martinis J. Chiral ground-state currents of interacting photons in a synthetic magnetic field. Nature Physics, 2017, 13(2): 146–151
57. Tai M E, Lukin A, Rispoli M, Schittko R, Menke T, Dan Borgnia , Preiss P M, Grusdt F, Kaufman A M, Greiner M. Microscopy of the interacting Harper-Hofstadter model in the two-body limit. Nature, 2017, 546(7659): 519–523
58. Zhou X, Wang Y, Leykam D, Chong Y D. Optical isolation with nonlinear topological photonics. New Journal of Physics, 2017, 19(9): 095002
59. Dobrykh D A, Yulin A V, Slobozhanyuk A P, Poddubny A N, Kivshar Y S. Nonlinear control of electromagnetic topological edge states. Physical Review Letters, 2018, 121(16): 163901
60. Rajesh C, Georgios T. Self-induced topological transition in phononic crystals by nonlinearity management. 2019, arXiv:1904.09466v1
61. Bender C M, Boettcher S. Real spectra in non-Hermitian Hamiltonians having PT symmetry. Physical Review Letters, 1998, 80(24): 5243–5246
62. Regensburger A, Bersch C, Miri M A, Onishchukov G, Christodoulides D N, Peschel U. Parity-time synthetic photonic lattices. Nature, 2012, 488(7410): 167–171
63. Yang Y, Peng C, Liang Y, Li Z, Noda S. Analytical perspective for bound states in the continuum in photonic crystal slabs. Physical Review Letters, 2014, 113(3): 037401
64. Zhen B, Hsu C W, Lu L, Stone A D, Soljačić M. Topological nature of optical bound states in the continuum. Physical Review Letters, 2014, 113(25): 257401
65. Malzard S, Poli C, Schomerus H. Topologically protected defect states in open photonic systems with non-Hermitian charge-conjugation and parity-time symmetry. Physical Review Letters,

2015, 115(20): 200402
66. Zeuner J M, Rechtsman M C, Plotnik Y, Lumer Y, Nolte S, Rudner M S, Segev M, Szameit A. Observation of a topological transition in the bulk of a non-Hermitian system. Physical Review Letters, 2015, 115(4): 040402
67. Zhen B, Hsu C W, Igarashi Y, Lu L, Kaminer I, Pick A, Chua S L, Joannopoulos J D, Soljačić M. Spawning rings of exceptional points out of Dirac cones. Nature, 2015, 525(7569): 354–358
68. Cerjan A, Raman A, Fan S. Exceptional contours and band structure design in parity-time symmetric photonic crystals. Physical Review Letters, 2016, 116(20): 203902
69. Bulgakov E N, Maksimov D N. Topological bound states in the continuum in arrays of dielectric spheres. Physical Review Letters, 2017, 118(26): 267401
70. Feng L, El-Ganainy R, Ge L. Non-Hermitian photonics based on parity-time symmetry. Nature Photonics, 2017, 11(12): 752–762
71. Kodigala A, Lepetit T, Gu Q, Bahari B, Fainman Y, Kanté B. Lasing action from photonic bound states in continuum. Nature, 2017, 541(7636): 196–199
72. Weimann S, Kremer M, Plotnik Y, Lumer Y, Nolte S, Makris K G, Segev M, Rechtsman M C, Szameit A. Topologically protected bound states in photonic parity-time-symmetric crystals. Nature Materials, 2017, 16(4): 433–438
73. El-Ganainy R, Makris K G, Khajavikhan M, Musslimani Z H, Rotter S, Christodoulides D N. Non-Hermitian physics and PT symmetry. Nature Physics, 2018, 14(1): 11–19
74. Kawabata K, Shiozaki K, Ueda M. Anomalous helical edge states in a non-Hermitian Chern insulator. Physical Review B, 2018, 98(16): 165148
75. Kunst F K, Edvardsson E, Budich J C, Bergholtz E J. Biorthogonal bulk-boundary correspondence in non-Hermitian systems. Physical Review Letters, 2018, 121(2): 026808
76. Lieu S. Topological phases in the non-Hermitian Su-Schrieffer-Heeger model. Physical Review B, 2018, 97(4): 045106
77. Pan M, Zhao H, Miao P, Longhi S, Feng L. Photonic zero mode in a non-Hermitian photonic lattice. Nature Communications, 2018, 9(1): 1308
78. Qi B, Zhang L, Ge L. Defect states emerging from a non-Hermitian flatband of photonic zero modes. Physical Review Letters, 2018, 120(9): 093901
79. Shen H, Zhen B, Fu L. Topological band theory for non-Hermitian Hamiltonians. Physical Review Letters, 2018, 120(14): 146402
80. Wang H F, Gupta S K, Zhu X Y, Lu M H, Liu X P, Chen Y F. Bound states in the continuum in a bilayer photonic crystal with TE-TM cross coupling. Physical Review. B, 2018, 98(21): 214101
81. Yao S, Song F, Wang Z. Non-Hermitian Chern bands. Physical Review Letters, 2018, 121(13): 136802
82. Yao S, Wang Z. Edge states and topological invariants of non-Hermitian systems. Physical Review Letters, 2018, 121(8): 086803
83. Chen X D, Deng W M, Shi F L, Zhao F L, Chen M, Dong J W. Direct observation of corner states in second-order topological photonic crystal slabs. 2018, arXiv:1812.08326
84. Ezawa M. Higher-order topological insulators and semimetals on the breathing kagome and pyrochlore lattices. Physical Review Letters, 2018, 120(2): 026801
85. Ezawa M. Minimal models for Wannier-type higher-order topological insulators and phosphorene. Physical Review B, 2018, 98(4): 045125
86. Ezawa M. Magnetic second-order topological insulators and semimetals. Physical Review B, 2018, 97(15): 155305
87. Ezawa M. Higher-order topological electric circuits and topological corner resonance on the breathing kagome and pyrochlore lattices. Physical Review B, 2018, 98(20): 201402
88. Geier M, Trifunovic L, Hoskam M, Brouwer P W. Second-order topological insulators and superconductors with an order-two crystalline symmetry. Physical Review B, 2018, 97(20): 205135
89. Khalaf E. Higher-order topological insulators and superconductors protected by inversion symmetry. Physical Review B, 2018, 97(20): 205136
90. Kunst F K, van Miert G, Bergholtz E J. Lattice models with exactly solvable topological hinge and corner states. Physical Review B, 2018, 97(24): 241405
91. Peterson C W, Benalcazar W A, Hughes T L, Bahl G. A quantized microwave quadrupole insulator with topologically protected corner states. Nature, 2018, 555(7696): 346–350
92. Schindler F, Cook A M, Vergniory M G, Wang Z, Parkin S S, Bernevig B A, Neupert T.Higher-order topological insulators. Science Advances, 2018, 4(6): eaat0346
93. van Miert G, Ortix C. Higher-order topological insulators protected by inversion and rotoinversion symmetries. Physical Review B, 2018, 98(8): 081110
94. Xie B Y, Wang H F, Wang H X, Zhu X Y, Jiang J H, Lu M H, Chen Y F. Second-order photonic topological insulator with corner states. Physical Review B, 2018, 98(20): 205147
95. Xie B Y, Su G X, Wang H F, Su H, Shen X P, Zhan P, Lu M H, Wang Z L, Chen Y F. Visualization of higher-order topological insulating phases in two-dimensional dielectric photonic crystals. Physical Review Letters, 2019, 122(23): 233903
96. Yasutomo O, Feng L, Ryota K, Katsuyuki W, Katsunori W, Yasuhiko A, Satoshi I. Photonic crystal nanocavity based on a topological corner state. 2018, arXiv:1812.10171
97. Călugăru D, Juričić V, Roy B. Higher-order topological phases: a general principle of construction. Physical Review B, 2019, 99(4): 041301
98. Hu H, Huang B, Zhao E, Liu W V. Dynamical singularities of Floquet higher-order topological insulators. 2019, arXiv:1905.03727v1
99. Armstrong J A, Bloembergen N, Ducuing J, Pershan P S. Interactions between light waves in a nonlinear dielectric. Physical Review, 1962, 127(6): 1918–1939
100. Kleinman D A. Nonlinear dielectric polarization in optical media. Physical Review, 1962, 126(6): 1977–1979
101. Adler E. Nonlinear optical frequency polarization in a dielectric. Physical Review, 1964, 134(3A): A728–A733
102. Miller R C. Optical second harmonic generation in piezoelectric crystals. Applied Physics Letters, 1964, 5(1): 17–19
103. Fejer M M, Magel G, Jundt D H, Byer R L. Quasi-phase-matched second harmonic generation: tuning and tolerances. IEEE Journal of Quantum Electronics, 1992, 28(11): 2631–2654
104. Yamada M, Nada N, Saitoh M, Watanabe K. First-order quasi-phase matched LiNbO3waveguide periodically poled by applying an external field for efficient blue second–harmonic generation.

Applied Physics Letters, 1993, 62(5): 435–436
105. Celebrano M, Wu X, Baselli M, Großmann S, Biagioni P, Locatelli A, De Angelis C, Cerullo G, Osellame R, Hecht B, Duò L, Ciccacci F, Finazzi M. Mode matching in multiresonant plasmonic nanoantennas for enhanced second harmonic generation. Nature Nanotechnology, 2015, 10(5): 412–417
106. Rubin M H, Klyshko D N, Shih Y H, Sergienko A V. Theory of two-photon entanglement in type-II optical parametric down-conversion. Physical Review A, 1994, 50(6): 5122–5133
107. Monken C H, Ribeiro P S, Pádua S. Transfer of angular spectrum and image formation in spontaneous parametric down-conversion. Physical Review A, 1998, 57(4): 3123–3126
108. Arnaut H H, Barbosa G A. Orbital and intrinsic angular momentum of single photons and entangled pairs of photons generated by parametric down-conversion. Physical Review Letters, 2000, 85(2): 286–289
109. Howell J C, Bennink R S, Bentley S J, Boyd R W. Realization of the Einstein-Podolsky-Rosen paradox using momentum- and position-entangled photons from spontaneous parametric down conversion. Physical Review Letters, 2004, 92(21): 210403
110. Harder G, Bartley T J, Lita A E, Nam S W, Gerrits T, Silberhorn C. Single-mode parametric-down-conversion states with 50 photons as a source for mesoscopic quantum optics. Physical Review Letters, 2016, 116(14): 143601
111. Carriles R, Schafer D N, Sheetz K E, Field J J, Cisek R, Barzda V, Sylvester A W, Squier J A. Imaging techniques for harmonic and multiphoton absorption fluorescence microscopy. Review of Scientific Instruments, 2009, 80(8): 081101
112. Grinblat G, Li Y, Nielsen M P, Oulton R F, Maier S A. Enhanced third harmonic generation in single germanium nanodisks excited at the anapole mode. Nano Letters, 2016, 16(7): 4635–4640
113. Sipe J E, Moss D J, van Driel H. Phenomenological theory of optical second- and third-harmonic generation from cubic centrosymmetric crystals. Physical Review B, 1987, 35(3): 1129–1141
114. Zhu S, Zhu Y, Ming N. Quasi-phase-matched third-harmonic generation in a quasi-periodic optical superlattice. Science, 1997, 278(5339): 843–846
115. Soavi G, Wang G, Rostami H, Purdie D G, De Fazio D, Ma T, Luo B, Wang J, Ott A K, Yoon D, Bourelle S A, Muench J E, Goykhman I, Dal Conte S, Celebrano M, Tomadin A, Polini M, Cerullo G, Ferrari A C. Broadband, electrically tunable third-harmonic generation in graphene. Nature Nanotechnology, 2018, 13(7): 583–588
116. Slusher R E, Hollberg L W, Yurke B, Mertz J C, Valley J F. Observation of squeezed states generated by four-wave mixing in an optical cavity. Physical Review Letters, 1985, 55(22): 2409–2412
117. Deng L, Hagley E W, Wen J, Trippenbach M, Band Y, Julienne P S, Simsarian J, Helmerson K, Rolston S, Phillips W D. Four-wave mixing with matter waves. Nature, 1999, 398(6724): 218–220
118. Bencivenga F, Cucini R, Capotondi F, Battistoni A, Mincigrucci R, Giangrisostomi E, Gessini A, Manfredda M, Nikolov I P, Pedersoli E, Principi E, Svetina C, Parisse P, Casolari F, Danailov M B, Kiskinova M, Masciovecchio C. Four-wave mixing experiments with extreme ultraviolet transient gratings. Nature, 2015, 520(7546): 205–208
119. Singh S K, Abak M K, Tasgin M E. Enhancement of four-wave mixing via interference of multiple plasmonic conversion paths. Physical Review B, 2016, 93(3): 035410
120. Zhang H, Virally S, Bao Q, Ping L K, Massar S, Godbout N, Kockaert P. Z-scan measurement of the nonlinear refractive index of graphene. Optics Letters, 2012, 37(11): 1856–1858
121. Alam M Z, De Leon I, Boyd R W. Large optical nonlinearity of indium tin oxide in its epsilon-near-zero region. Science, 2016, 352(6287): 795–797
122. Ozawa T, Price H M, Amo A, Goldman N, Hafezi M, Lu L, Rechtsman M C, Schuster D, Simon J, Zilberberg O, Carusotto I. Topological photonics. Reviews of Modern Physics, 2019, 91(1): 015006
123. Berry M V. Quantal phase factors accompanying adiabatic changes. Proceedings of the Royal Society of London, Series A, Mathematical and Physical Sciences, 1802, 1984(392): 45–57
124. Pancharatnam S. Generalized theory of interference and its applications. Proceedings of the Indian Academy of Sciences, Section A, Physical Sciences, 1956, 44(6): 398–417
125. Skirlo S A, Lu L, Igarashi Y, Yan Q, Joannopoulos J, Soljačić M. Experimental observation of large Chern numbers in photonic crystals. Physical Review Letters, 2015, 115(25): 253901
126. Lu L, Wang Z, Ye D, Ran L, Fu L, Joannopoulos J D, Soljačić M. Experimental observation of Weyl points. Science, 2015, 349 (6248): 622–624
127. Xiao M, Lin Q, Fan S. Hyperbolic Weyl point in reciprocal chiral metamaterials. Physical Review Letters, 2016, 117(5): 057401
128. Lin Q, Xiao M, Yuan L, Fan S. Photonic Weyl point in a two-dimensional resonator lattice with a synthetic frequency dimension. Nature Communications, 2016, 7(1): 13731
129. Fang C, Weng H, Dai X, Fang Z. Topological nodal line semimetals. Chinese Physics B, 2016, 25(11): 117106
130. Lu L, Fu L, Joannopoulos J D, Soljačić M. Weyl points and line nodes in gyroid photonic crystals. Nature Photonics, 2013, 7(4): 294–299
131. Yang B, Guo Q, Tremain B, Liu R, Barr L E, Yan Q, Gao W, Liu H, Xiang Y, Chen J, Fang C, Hibbins A, Lu L, Zhang S. Ideal Weyl points and helicoid surface states in artificial photonic crystal structures. Science, 2018, 359(6379): 1013–1016
132. Chen W J, Jiang S J, Chen X D, Zhu B, Zhou L, Dong J W, Chan C T. Experimental realization of photonic topological insulator in a uniaxial metacrystal waveguide. Nature Communications, 2014, 5(1): 5782
133. Slobozhanyuk A P, Khanikaev A B, Filonov D S, Smirnova D A, Miroshnichenko A E, Kivshar Y S. Experimental demonstration of topological effects in bianisotropic metamaterials. Scientific Reports, 2016, 6(1): 22270
134. Shalaev M I, Walasik W, Tsukernik A, Xu Y, Litchinitser N M. Robust topologically protected transport in photonic crystals at telecommunication wavelengths. Nature Nanotechnology, 2019, 14(1): 31–34
135. Chen X D, Zhao F L, Chen M, Dong J W. Valley-contrasting physics in all-dielectric photonic crystals: orbital angular momentum and topological propagation. Physical Review B, 2017, 96(2): 020202

136. Chen X D, Shi F L, Liu H, Lu J C, Deng W M, Dai J Y, Cheng Q, Dong J W. Tunable electromagnetic flow control in valley photonic crystal waveguides. Physical Review Applied, 2018, 10(4): 044002
137. He M, Zhang L, Wang H. Two-dimensional photonic crystal with ring degeneracy and its topological protected edge states. Scientific Reports, 2019, 9(1): 3815
138. Ma T, Khanikaev A B, Mousavi S H, Shvets G. Guiding electromagnetic waves around sharp corners: topologically protected photonic transport in metawaveguides. Physical Review Letters, 2015, 114(12): 127401
139. Chen W J, Xiao M, Chan C T. Photonic crystals possessing multiple Weyl points and the experimental observation of robust surface states. Nature Communications, 2016, 7(1): 13038
140. Chen Y, Chen H, Cai G. High transmission in a metal-based photonic crystal. Applied Physics Letters, 2018, 112(1): 013504
141. El-Kady I, Sigalas M, Biswas R, Ho K, Soukoulis C. Metallic photonic crystals at optical wavelengths. Physical Review B, 2000, 62(23): 15299–15302
142. Gao F, Gao Z, Shi X, Yang Z, Lin X, Xu H, Joannopoulos J D, Soljačić M, Chen H, Lu L, Chong Y, Zhang B. Probing topological protection using a designer surface plasmon structure. Nature Communications, 2016, 7(1): 11619
143. Gao W, Yang B, Tremain B, Liu H, Guo Q, Xia L, Hibbins A P, Zhang S. Experimental observation of photonic nodal line degeneracies in metacrystals. Nature Communications, 2018, 9(1): 950
144. Gao F, Xue H, Yang Z, Lai K, Yu Y, Lin X, Chong Y, Shvets G, Zhang B. Topologically protected refraction of robust kink states in valley photonic crystals. Nature Physics, 2018, 14(2): 140–144
145. Karch A. Surface plasmons and topological insulators. Physical Review B, 2011, 83(24): 245432
146. Hafezi M, Mittal S, Fan J, Migdall A, Taylor J M. Imaging topological edge states in silicon photonics. Nature Photonics, 2013, 7(12): 1001–1005
147. Mittal S, Ganeshan S, Fan J, Vaezi A, Hafezi M. Measurement of topological invariants in a 2D photonic system. Nature Photonics, 2016, 10(3): 180–183
148. Harari G, Bandres M A, Lumer Y, Rechtsman M C, Chong Y D, Khajavikhan M, Christodoulides D N, Segev M.Topological insulator laser: theory. Science, 2018, 359(6381): eaar4003
149. Bandres M A, Wittek S, Harari G, Parto M, Ren J, Segev M, Christodoulides D N, Khajavikhan M. Topological insulator laser: experiments. Science, 2018, 359(6381): eaar4005
150. Midya B, Zhao H, Feng L. Non-Hermitian photonics promises exceptional topology of light. Nature Communications, 2018, 9(1): 2674
151. Barik S, Karasahin A, Flower C, Cai T, Miyake H, DeGottardi W, Hafezi M, Waks E. A topological quantum optics interface. Science, 2018, 359(6376): 666–668
152. Blanco-Redondo A, Bell B, Oren D, Eggleton B J, Segev M. Topological protection of biphoton states. Science, 2018, 362 (6414): 568–571
153. Piper J R, Fan S. Total absorption in a graphene monolayer in the optical regime by critical coupling with a photonic crystal guided resonance. ACS Photonics, 2014, 1(4): 347–353
154. Gan X, Mak K F, Gao Y, You Y, Hatami F, Hone J, Heinz T F, Englund D. Strong enhancement of light-matter interaction in graphene coupled to a photonic crystal nanocavity. Nano Letters, 2012, 12(11): 5626–5631
155. Heeger A J, Kivelson S, Schrieffer J R, Su W P. Solitons in conducting polymers. Reviews of Modern Physics, 1988, 60(3): 781–850
156. Su W P, Schrieffer J R, Heeger A J. Solitons in Polyacetylene. Physical Review Letters, 1979, 42(25): 1698–1701
157. Miri M-A, Alù A. Exceptional points in optics and photonics. Science, 2019, 363(6422): eaar7709
158. Gupta S K, Zou Y, Zhu X Y, Lu M H, Zhang L, Liu X P, Chen Y F. Parity-time symmetry in Non-Hermitian complex media. 2018, arXiv:1803.00794
159. Lee T E. Anomalous edge state in a non-Hermitian lattice. Physical Review Letters, 2016, 116(13): 133903
160. Ghatak A, Das T. New topological invariants in non-Hermitian systems. Journal of Physics Condensed Matter, 2019, 31(26): 263001
161. St-Jean P, Goblot V, Galopin E, Lemaître A, Ozawa T, Le Gratiet L, Sagnes I, Bloch J, Amo A. Lasing in topological edge states of a one-dimensional lattice. Nature Photonics, 2017, 11(10): 651–656
162. Parto M, Wittek S, Hodaei H, Harari G, Bandres M A, Ren J, Rechtsman M C, Segev M, Christodoulides D N, Khajavikhan M. Edge-mode lasing in 1D topological active arrays. Physical Review Letters, 2018, 120(11): 113901
163. Zhao H, Miao P, Teimourpour M H, Malzard S, El-Ganainy R, Schomerus H, Feng L. Topological hybrid silicon microlasers. Nature Communications, 2018, 9(1): 981
164. Ota Y, Katsumi R, Watanabe K, Iwamoto S, Arakawa Y. Topological photonic crystal nanocavity laser. Communications on Physics, 2018, 1(1): 86
165. Haldane F D M. Model for a quantum Hall effect without Landau levels: condensed-matter realization of the “parity anomaly”. Physical Review Letters, 1988, 61(18): 2015–2018
166. Schmidt J, Marques M R G, Botti S, Marques M A L. Recent advances and applications of machine learning in solid-state materials science. NPJ Computational Materials, 2019, 5(1): 83
167. Pilozzi L, Farrelly F A, Marcucci G, Conti C. Machine learning inrerse problem for topological photonics. Communications Physics, 2018, 1(1): 57
168. Long Y, Ren J, Li Y, Chen H. Inverse design of photonic topological state via machine learning. Applied Physics Letters, 2019, 114(18): 181105
169. Barth C, Becker C. Machine learning classification for field distributions of photonic modes. Communications on Physics, 2018, 1(1): 58
170. Fano U. Effects of configuration interaction on intensities and phase shifts. Physical Review, 1961, 124(6): 1866–1878
171. Limonov M F, Rybin M V, Poddubny A N, Kivshar Y S. Fano resonances in photonics. Nature Photonics, 2017, 11(9): 543–554
172. Miroshnichenko A E, Flach S, Kivshar Y S. Fano resonances in nanoscale structures. Reviews of Modern Physics, 2010, 82(3): 2257–2298
173. Luk’yanchuk B S, Miroshnichenko A E, Kivshar Y S. Fano resonances and topological optics: an interplay of far- and near-

field interference phenomena. Journal of Optics, 2013, 15(7): 073001
174. Gao W, Hu X, Li C, Yang J, Chai Z, Xie J, Gong Q. Fano-resonance in one-dimensional topological photonic crystal heterostructure. Optics Express, 2018, 26(7): 8634–8644
175. Zangeneh-Nejad F, Fleury R. Topological Fano resonances. Physical Review Letters, 2019, 122(1): 014301
176. Liang G Q, Chong Y D. Optical resonator analog of a two-dimensional topological insulator. Physical Review Letters, 2013, 110(20): 203904

Hongfei Wang is a Ph.D. candidate in the Department of Materials Science and Engineering at Nanjing University. He spent his bachelor time at Anhui University during 2011–2015. His research topics include topological photonics, non-Hermitian photonics, and computational physics.

Dr. **Samit Kumar Gupta** received his Ph.D. in 2016 from the Department of Physics, Indian Institute of Technology Guwahati, India. Afterward, in 2017 he joined the College of Engineering and Applied Sciences, National Laboratory of Solid State Microstructures, Nanjing University as a Postdoc Fellow. His research interests include fundamental and applied aspects of nonlinear optics, nonlinear waves, non-Hermitian physics, and topological photonics.

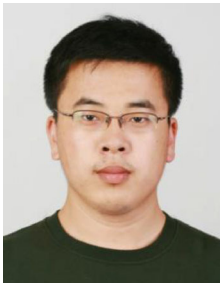

Dr. **Biye Xie** spent his bachelor time at the University of Science and Technology of China. He received his Ph.D. degree in Physics from the University of Hong Kong, China. His research interest includes topological photonics, topological phononics, metamaterials, and quantum information.

Prof. **Minghui Lu** received his Ph.D. degree from Nanjing University in 2007. He is an Associate Professor at Nanjing University since 2009 and a Professor in 2013. He had been a visiting scholar at SIMES, Stanford University during 2011–2012. His current research interests mainly focus on fundamental study of photonic and acoustic artificial structures and metamaterials as well as their related applications.